Slag-Limestone Blends for Sustainable Concrete

By

Pui Shan Tina Kwok (MUR)

Fourth-year undergraduate project
In Group D, 2012/2013

Technical abstract

Portland cement (PC) has long been playing a critical role in civil and structural engineering due to its excellent mechanical strength. The issue associated with PC is its carbon dioxide emission (~7% globally) and extensive energy consumption during the manufacturing process. With the rapid growth in infrastructure and structures in developing countries, the global cement production is expected to double to 7.2 billion tonnes by 2050. In some European countries, PC with up to 40% limestone is employed; CEMII/B-L cement contains up to 25% of limestone and has a 28-day design compressive strength is 42.5MPa. Recently, research work has been conducted on the development of sustainable concrete using limestone with AAS, hence mixing an extracted mineral with an industrial by-product respectively. The objectives of the work were to investigate the impact of high volume replacement of the slag by limestone on the compressive strength and shrinkage of cement and concrete cube samples. The activation of the slag blends by different types and dosages of alkalis was also investigated focusing on more sustainable alkalis than those usually used. So basically using sodium carbonate (Na_2CO_3) and magnesium oxide (MgO) instead of sodium hydroxide (NaOH). The effect of different compositions was examined in cement pastes as it gave more pronounced impacts. Selected samples from the cement paste work were then tested in concrete samples. The shrinkage performance was benchmarked against the standard CEM III cement-slag blends in 1:1 ratio.

In 5% Na_2CO_3 activated slag, the early unconfined compressive strength (UCS) dropped by 47% to 13.7 MPa as 20% of GGBS was replaced by limestone, due to the reduction in blend pH. However, the two mixes achieved similar 28-day UCS ~50 MPa. The denser structure due to the limestone filling effect compensated the strength lost from the reduction in GGBS content. As the limestone content continued to increase, both early and late strengths dropped due to the dilution effect. Since Na_2CO_3 is a relatively mild alkali activator, the limestone only acted as an inert filler in this set of mixes, and possibly source of Ca for C-(A)-S-H. In the context of shrinkage behaviour, 20% and 50% replacement of slag by limestone led to 19% and 64% increased in drying shrinkage respectively. Scanning electron microscopy analyses revealed an increase in the density of microcracks with limestone content.

The 5% NaOH activated slag gave a higher early strength for all slag to limestone ratios, but yielded a lower later strength due to its more porous structure and the lack of Na_2CO_3 which catalyses the consumption of Ca in limestone for the formation of C-(A)-S-H. Mixes with GGBS:limestone 4:1 ratio had 28-day UCS of 40 MPa respectively. As 50% of slag was replaced by limestone, the reduction in compressive strengths for NaOH- and Na_2CO_3-

activated slag were 18.5% and 26.9% respectively. The reasons behind were two-folds. First, due to the more porous structure of NaOH activated slag, the filling effect of the limestone powder was more pronounced. Secondly, in the presence of NaOH, strength contributing and shrinkage restraining crystalline $Ca(OH)_2$ was formed from the limestone. Further, the high early strength of NaOH activated slag enabled rapid uptake of free water and the formation of calcium silicate hydrated (CSH) which filled the voids and reduced the overall pore volume for shrinkage. 5% NaOH activated slag with GGBS:Limestone 4:1 ratio had a 28-day shrinkage strain 76% smaller than that of Na_2CO_3 activated slag. In addition, no surface cracking was observed over the 28-day period of testing.

Cement pastes with compressive strength in the range of 40-50 MPa is expected to give a concrete strength of ~30+ MPa. In order to improve the mechanical properties, combinations of activators were tested on mixes with 80% slag and 20% limestone. It was validated that slag activated by a combination of NaOH and Na_2CO_3 yielded higher strength at all ages than NaOH or Na_2CO_3 alone, since both high initial pH values and less porous structure can be attained. 1.5% NaOH + 3.5% Na_2CO_3 activated slag with GGBS:Limestone 4:1 ratio had 4-day and 28-day UCS of 31 MPa and 53 MPa respectively. The 1.5% replacement of Na_2CO_3 by NaOH also reduced the 28-day drying shrinkage by 47%, yet, its shrinkage remained 80% higher than the CEM III paste. It was also reported that Na_2CO_3 catalyses the consumption of limestone to form C-(A)-S-H. However, the increase of Na_2CO_3 from 5% to 15% led to a drop of 28-day strength from 50 MPa to 30 MPa due to the retardation effect and formation of strength detrimental gaylussite and thermonatrite.

The addition of MgO was tested on mixes with 4:1 slag-limestone pastes. In Na_2CO_3 activated-slag, there was a 43% upon at the 4-day strength for 10% MgO addition due to the higher pH attained. There was little impact on later strength, regardless of the type of activator used, due to the compensation of strength from formation of MAH by the strength loss from the reduction in limestone filler. The effect of MgO was more significant in drying shrinkage reduction due to the expansive MAH and $Mg(OH)_2$. A 24% reduction in drying shrinkage was observed, with little surface cracking and no microcracks detected on 28-day.

This work highlighted that the incorporation of high volume limestone in alkali-activated slag is viable and beneficial depending on the nature and dosage of the activators used, in the context of mechanical strength and shrinkage reduction. These formulations are encouraging as they have minimal carbon dioxide emissions and costs in comparison to PC. The highest concrete strength attained in this work was 37.5 MPa, which was only slightly below ACI standard of high-strength concrete.

Table of Contents

1 Introduction

1.1 Background

Concrete is the second most widely used material globally after water (Sidney 2011). It is the foundation of the built environment from our homes to the roads. Portland cement (PC) was considered to be the best building material for its high mechanical strength. However, ordinary PC does not only have insufficient durability performance and low resistance towards chemical attacks, the cement industry is also one of the most energy-consuming and greenhouse gases emitting industries and is responsible for 7% of the global carbon dioxide emissions (Foong 2009). The urge for materials with less embodied energy and carbon footprint stimulated research on developing new and sustainable alternatives or blended cements with lower embodied energy to cope with the rapidly growing cement and concrete demand which is expected to double by 2050, due to the rapid structural and infrastructural development in developing countries. Blended cements, in which a percentage of PC is substituted with either slag and other mineral additives such as limestone and silica fume, are now commonly used, and which reduce the production of PC, as well as enhance the performance. The only type of cement which excludes PC is alkali activated slag (AAS). Interest in AAS increased over the years due to its low embodied energy in production, superior mechanical performance and chemical resistance, although serious issues associated with significant shrinkage and carbonation have limited its application in construction. As the global annual production of slag suitable for use in cement is only 250 million tonnes, which is far less than the current cement consumption of 3.6 billion tonnes worldwide, it would make sense to blend the slag with other minerals, which are more widely available like limestone.

Limestone is one of the minerals widely used in binary or tertiary cement blends. It was identified as an improver of the pore structure and the hydration rate by acting as an inert filler for PC by decreasing the gel porosity. Limestone is also a highly sustainable source of minerals and CEMII/B-L cement contains up to 25% of limestone. However, the influence of limestone in Alkali-activated slag is yet to be investigated. Recently, Mosesons (2012) suggested that high volume replacement of Na_2CO_3 activated slag by limestone would yield a compatible mechanical strength to PC. He also suggested that limestone was one of the calcium sources for the production of the Calcium-(aluminimum)-silicate-hydrates (C(A)SH)

as the hydration product, under the presence of Na_2CO_3 catalyst. The effect of limestone in shrinkage of AAS is yet to be addressed. This has led to the initiation of this research work to investigate the effect of adding high volume limestone into AAS on the resulting mechanical and shrinkage performance. The effect of the types and dosages of activators, as well as the addition of reactive MgO as an alkali activator and an expansive additive, was also examined.

1.2 Aims and objectives

The aim of the project was to investigate the mechanical properties and shrinkage reduction of alkali-activated slag with high volume limestone content. The objectives of the work were to assess the effect of

- High volume replacement of GGBS by limestone
- Activation of slag and limestone mixes by different types and dosage of alkalis – Na_2CO_3 NaOH.
- Small addition of MgO

The testing began with cement pastes, as this offered more pronounced effects on the variation of mixes compositions and selected mixes with the highest compressive strengths were then tested as concrete. Microstructural analyses were used to explain some of the observations made and to assist in understanding the various effects of variables.

1.3 Structure of report

This report is divided into 6 chapters. Chapter 1 is an introduction, providing a background to the problem, motivation of this research, as well as the aims and objectives. Chapter 2 is the literature review on the main materials used in this project: Slag, Sodium hydroxide, Sodium carbonate, limestone and magnesium oxides. The durability issue associated with the use of alkali-activated slag is also discussed. Chapter 3 outlines the materials and experimental methods used. Chapter 4 presents the analysed results from the experiments alongside with suggested reasons for the effects. Chapter 5 concludes the findings drawn from this research project, recommends future works and comments on the risk assessment. Chapter 6 provides the list of references used in this report.

2 Literature review

This chapter summarises and reviews the relevant literatures on research work and other information published starting with a general overview on the sustainability of concrete. Relevant information on GGBS, activators – sodium hydroxide and sodium carbonate, limestone and magnesium oxide is then presented and discussed.

2.1 Sustainable concrete

The Cement and Concrete Institute (Sakai 2011) defined sustainable concrete as: "Concrete has a low embodied energy and a significant number of inherent characteristics which contribute to sustainability of concrete structures". Sustainability can be achieved in various ways. To a large extent, research and applications of sustainable concrete has focused on the incorporation of low carbon footprint cemenetitious or pozzolanic industrial by-products into the PC. The most commonly used extender is ground granulated blastfurnace slag (GGBS). In recent years, an increasing interest in using slag alone with alkali activators was seen, due to its high sustainability. Fillers materials like fine limestone powder are also widely used. In Europe, up to 25% limestone is allowed in blended cement. The average greenhouse gases emission of PC, GGBS and limestone are 913, 67 and 75 kg of carbon dioxide equivalent (CO_2e) per tonnes of materials respectively (MPA 2011). Improving concrete durability and mechanical strength are also critical in the development of sustainable concrete since poorly designed concrete leads to serious deterioration and consequential re-consturction. Use of mineral admixtures, like magnesium oxides (MgO), has also risen in popularity. The Baishan Dam in China was a successful example, where 4-8% of MgO addition greatly reduced shrinkage.

2.2 Alkali activated slag (AAS)

Slag was the first cementitious material activated by alkalis, and ground granulated blast furnace slag (GGBS) was the most suitable due to the its latent hydraulic properties. The development of AAS was mainly contributed by Purdon in 1940s (Fernando 2008). His results led to the conclusion that NaOH catalyses the hydration process of GGBS. AAS is competitive with ordinary PC in performance and cost. while GGBS manufacturing process is more environmentally-friendly.

Slag is an industrial by-product from the combustion of metal ores, mostly from steel production. GGBS is commonly found in United Kingdom. It is obtained by quenching

2000°C molten iron slag from blast furnace in water to give a glassy product. To maintain high level of hydraulic properties, slag must be cooled as soon as it leaves the furnace. Upon drying, it is grounded to fine powder. The production of GGBS only accounts for 7% of the greenhouse gasses emissions of PC (MPA, 2011). The typical composition of GGBS is as shown in Table 2-1. Like PC, its content is calcium and silicon rich, and most of calcium oxide (CaO) in GGBS is found in the found of calcium silicate, calcium aluminate and calcium aluminosilicate. However, these compounds in PC are in tricalcium silicate field while those in GGBS products are in diclacium silicate field (ACI 2000).

Components (as Oxides)	SiO_2	Al_2O_3	CaO	MgO	Fe_2O_3	SO_3	L.O.1
GGBS (% by weight)	40.0	13.5	39.2	3.6	1.8	0.2	0
PC (% by weight)	21.1	4.6	65.1	4.5	2.0	2.8	1.4

Table 2-1 Typical GGBS and CEM I composition (ASTM C989 Slag Activity)

Since GGBS is a glassy product, it is more reactive than other admixtures commonly used in PC mixes, for instance fly ash. Slag also has latent hydraulic properties, whereby the material reacts with water to form Calcium-Silicate-Hydrates (CSH). Oolarisation effect of OH^- ions in water breaks down the Si-O, Al-O and Ca-O bonds to form ions which react and form CSH. Due to the relatively high aluminium content, Calcium-Aluminium-Silicate-Hydrates (C(A)SH) also forms. However, the hydration process of GGBS in water is very slow, which initiated the use to alkalis to accelerate strength development.

Slag is an attractive alternative to PC. Besides low environment impact and high sustainability, the addition of GGBS improves late strength, workability, pumpability and placeability characteristics of concrete, as well as enables low heat of hydration and low water-to-slag ratio, high chemical resistance. However, the application of GGBS in concrete is restricted to 50% in most industrial application due to its drawbacks from the quick setting and high resulting shrinkage. Collins and Sanjayan (2000 & 2001) reported that its shrinkage was about two times greater than that in PC concrete, as seen in Figure 2-1 (a). The shrinkage mechanisms of ASS are yet to be well understood and different mechanisms or causes have been proposed over the years. Collins and Sanjayan reported that the early strength is critical to the shrinkage performance, as Chi (2012) stated that most of the drying shrinkage takes place during early stage. Low hydration rate leads to evaporation of free water at early stage, hence, leaving open pores and collapsing of CSH. The lack of crystalline compounds in AAS also causes high shrinkage in drying condition, as crystalline compounds can restrain CSH collapsing upon water removal. Collins and Sanjayan (2000 & 2001) also reported that the

pore distribution and CSH gel characteristics also have critical influences on the magnitude of drying shrinkage. Shi (1996) stated that AAS has a lower porosity than PC. As the smaller the pore radius is, the higher the capillary tensile force set up in meniscus. This leads to higher shrinkage. However, an increase in total pore volume gives extra space for the shrinkage and cracking upon drying (Shi 2006).

Cinotto (2013) also discovered that AAS has higher autogenous shrinkage than PC. At lower water-to-cement ratios, water in the mixes is rapidly drawn into the matrix leading to localized drying of internal capillary pores. The high surface tension in capillary leads to autogenous shrinkage and cracking. This shrinkage cannot be prevented by casting nor curing methods, but the w/c ratios.

The high shrinkage results in severe cracking in AAS concrete (AASC) than in ordinary Portland cement concrete (OPCC), as shown in Figure 2-1 (b). Expansive agents like ettringite and CaO, have been used in Portland cement to compensate shrinkage. However, AAS lacks $Ca(OH)_2$ for the formation of ettringite. Nonetheless, CaO and ettringite types expansive agents are water-soluble and react with alkalis. Therefore, other expansive agents, like MgO, should be considered in shrinkage reduction of slag and limestone mixes.

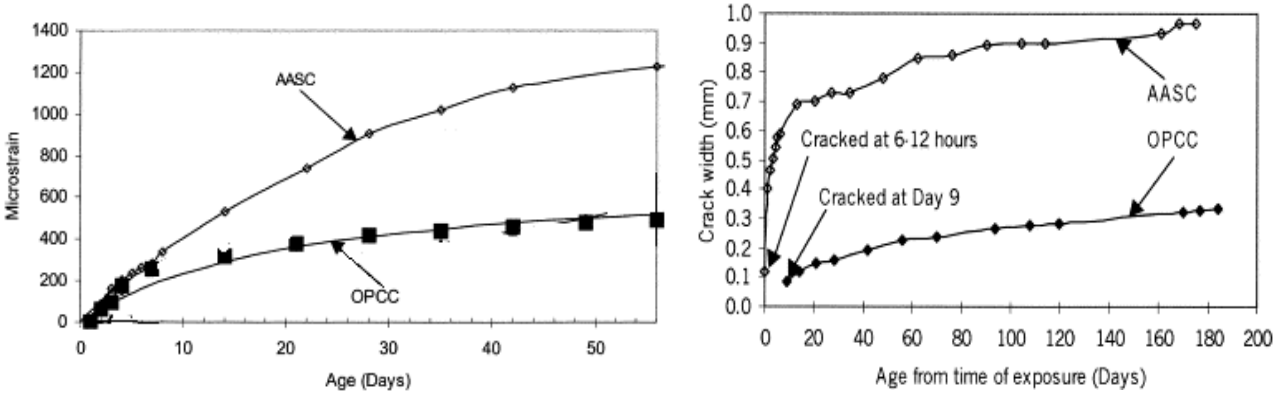

(a) (b)

Figure 2-1 (a) Comparison of drying shrinkage strain development of AASC and OPCC prisms exposed to 23°C temperature and 50% RH (Collins and Sanjayan 2001), and (b) compare the crack width development in AASC and OPCC (Collin & Sanjayan 2000)

2.3 Alkali activators

Alkali activators are applied to slag to stimulate the early stage hydration process by providing OH^- ions. Taylor (1997) also stated that an alkaline environment break down the coating formed on the surface of slag grains which prevent further hydration. In addition, the alkalis control the nature of the CSH formed by affecting the pH of the pore solutions. In

highly alkaline solution, the solubility of Ca^{2+} drops as $Ca(OH)_2$ is more favourable thermal-dynamically resulting in the formation of C-S-H with relatively lower Ca to Si ratio. The dissolution of slag in alkalis also promotes the incorporation of aluminium in the CSH (C(A)SH) and formation of hydrotalcite-like phases (Gruskovnjak 2006).

Sodium hydroxide (NaOH) and sodium carbonate (Na_2CO_3) are two of the effective alkalis. NaOH is more commonly used commercially due to its high alkalinity. With12.4% dosage of Na_2O in 100ml solution, NaOH and Na_2CO_3 solution have pH of 14.6 and 12.6 respectively. high alkalinity in NaOH results in higher early strength, while the presence of the CO_3^{2-} anions in Na_2CO_3 yields a higher late strength. Malolepszy (1986) found that Na_2CO_3 is especially suitable for slag rich in Calcium magnesium silicate (C_2MS), while NaOH is good for slag rich in Calcium aluminium silicate (C_2AS). The composition of minor hydration products and porosity depends on the activators used. Jolicoeur et al (1992) reported that the combination of NaOH and Na_2CO_3 yielded higher early strengths than NaOH or Na_2CO_3 alone.

Parameswaran et al (1986) suggested that the optimum activator dosage for slag ranges between 2% and 5%, and the higher the better. Wang (1994) stated that beyond an optimal alkali dosage, the free alkali increases efflorescence and brittleness of cement. Reddy et al (2006) observed the formation of alkali-silicate gel (gyrolite) in excess alkalis. When gyrolite gel comes in contact with water, it swells and expands which results in cracking of the cement paste matrix and hence a drop in compressive strength.

Commercial NaOH is manufactured via the hydrolysis of brine solution and solid NaOH is obtained by cooling the molten caustic soda. Puertas et al (2004) noted that NaOH activated slag resulted in hydration products with higher Al/Si molar ratio. Schilling et al (1994) and Shi and Day (1996) reported that calcium-aluminium-silicate-hydrates (C_2ASH_8) and Calcium-aluminium-hydrates (C_4AH_{13}) are the minor hydration products. C_2ASH_8 is an AFm phase which has interlayers of aluminosilicate anion. AFm phase refers to “alumina ferric oxide, monosulphate” phase which is a family of hydrated calcium aluminates with a hydrocalumite-like structure (Matschei et al. 2007). If MgO content in slag is high, the formation of magnesium aluminate hydrate (M_4AH_{13}) is more favourable than C_4AH_{13}.

Haha et al (2010) reported that the CSH gel presence in NaOH activated slag is more crystalline and contains less water leads to coarser capillary porosity and more porous

structure, hence, lower late strength. Figure 2-2 shows the microstructure of NaOH-activated slag. At 1 day, the structure of NaOH-activated slag still seems relatively loose.

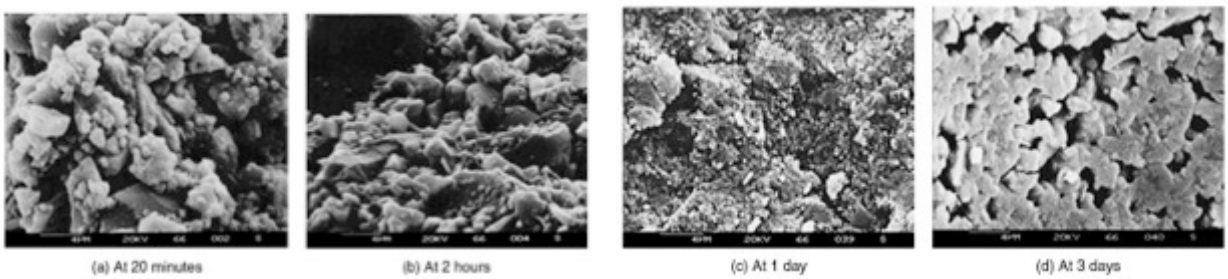

Figure 2-2 Microstructure of NaOH activated slag (Shi 1997)

Compared to NaOH, Na_2CO_3 is a more sustainable activator as it can be obtained from natural resources without energy intensive electrolysis reactions. Shi 2006 stated that Na_2CO_3 exists as salts with chlorides and sulphate ions that can be found in alkaline lake sand marshes. Na_2CO_3 is considered as a mild alkali as it is relatively insoluble in water and the initial retardation process (Jimenez and Puertas, 2003). These lead to a longer setting time and a lower early strength in Na_2CO_3 activated slag. Yet, the presence of CO_3^{2-} gives a higher later strength, as seen in Figure 2-4 (a). Voinvitch and Dron (1976) stated that tricalcium-aluminium-carbonate-hydrates ($C_3A.CaCO_3.12H_2O$) is the minor hydration product found in Na_2CO_3 activated slag. Figure 2-3 shows the microstructure of Na_2CO_3-activated slag at the early stage of hydration and shows that Na_2CO_3 gives a relatively denser microstructure at 1 day.

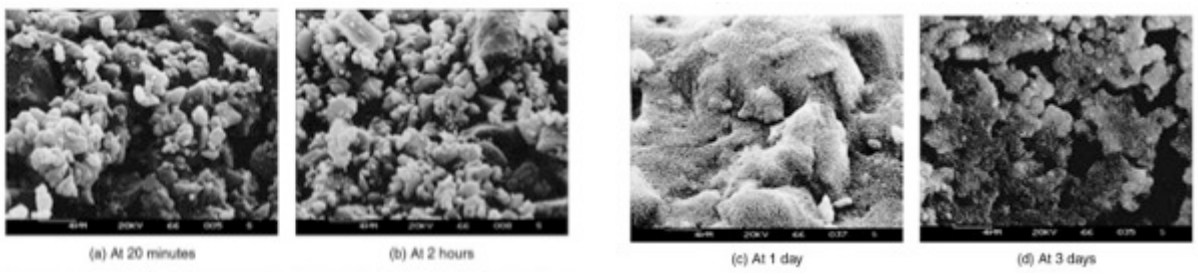

Figure 2-3 Microstructure of Na_2CO_3 activated slag (Shi 1997)

Shi (1996) examined the pore structure of slag activated by NaOH and Na_2CO_3. As seen in Figure 2-4 (b), NaOH actived slag is generally more porous and shows less uniformity in the distribution of pores than Na_2CO_3 activated slag (Figure 2-4 (c)). As seen from Figure 2-4 (b), at 3- and 7-day, there was a rapid reduction in the cumulative pore volume with an increase in the pore radius which results in a higher strength than NaOH activated slag at later stage.

Figure 2-5 shows the relationship between compressive strength and porosity of slag activated by Na_2CO_3 and NaOH. Pore structure is one of the determinants of shrinkage performance as discussed. The higher the total pore volume, the more water loss from the pore solution and the more space for shrinkage and cracking. Limited research was performed on the shrinkage performance of Na_2CO_3 activated slag, as oppose to that activated by NaOH and waterglass. Nonetheless, dosage control is particularly critical for Na_2CO_3 activated slag. The formation of gaylussite ($Na_2Ca(CO_3)_2$) and thermonatrite ($NaCO_3.H_2O$) from excessive Na_2CO_3 is detrimental to strength and leads to poor hydraulic stability:

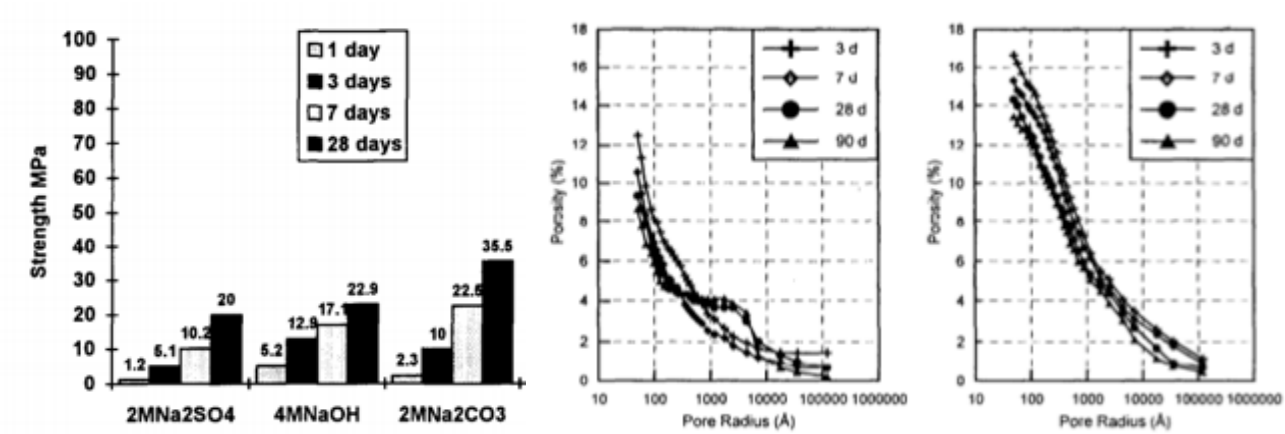

(a) (b) (c)

Figure 2-4 (a) Comparing compressive strengths of NaOH and Na2CO3 activated slag (Wang et al 1994) (b) Cumulative pore volume of Na2CO3 activated slag (Shi 1996) (c) Cumulative pore volume of NaOH activated slag (Shi 1996)

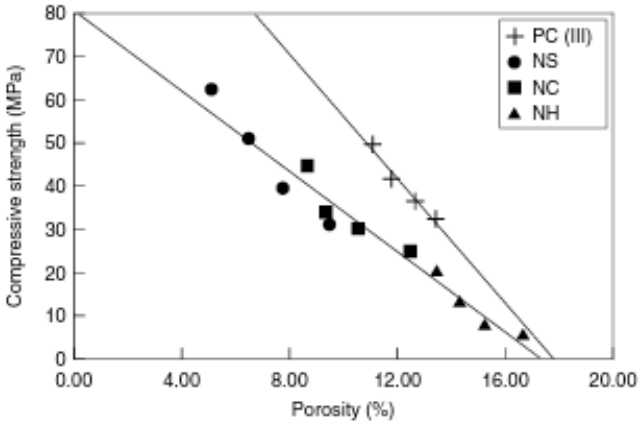

Figure 2-5 The relationship between compressive strength and porosity for slag activated by different activators; NC = Na_2CO_3, NH = NaOH; NS = sodium silicate

2.4 Limestone

Limestone is a sedimentary rock composed of calcite and aragonite, which are different forms of calcium carbonate ($CaCO_3$). The low greenhouse gases emission in production and abundance also makes it a highly sustainable additives or replacement of cement in concrete.

In the European standard EN 197-1 (CEN 2000), up to 25% limestone is allowed in cement. Recent research reveals that, to various extents, limestone is active both physically and chemically (Moseson 2012). Traditionally, limestone in concrete is considered to be an inert filling material that provides surfaces for the precipitation of Portlandite grains. The stimulation effect enables more homogenous distribution of CSH, and hence a higher early strength and less open pore structure. Sellevold et al (1982) showed that an incorporation of 12% $CaCO_3$ gave finer pore structures as well as reduction in total pore volume. Dewiler (1995) found that the wide particle size distribution fills the gaps between particles which reduces the water demand. Chemically, with the presence of highly alkaline hydroxide solution, $CaCO_3$ transforms into calcium hydroxide ($Ca(OH)_2$) which contributes to strength development. The crystalline phase $Ca(OH)_2$ also restraints the collapse of CSH gel upon water removal

$$CaCO_3 + 2NaOH \rightarrow Ca(OH)_2 + Na_2CO_3$$

Research on the addition of limestone in PC and concrete has been well-established, while the application of limestone in alkali-activated slag is relatively unknown. Recently, Moseson (2012) examined the impact on compressive strength and modulus of elasticity of AAS with high volume limestone replacement. Cement pastes with 50% slag, 50% limestone, 5% Na_2CO_3 and a water-to-cement ratio of 0.25 achieved a 28-day strength of 41.6MPa. By reducing the water-to-demand ratio to 0.18 without plasticiser, the 28-day strength increased to 51.2 MPa. The addition of limestone was shown to optimize the slow strength development in Na_2CO_3 activated slag. Moseson also reported that $CaCO_3$ reacts with Magnesium ions (Mg^{2+}) in slag to form dolomite ($CaMg(CO_3)_2$). The Ca^{2+} presence in dolomite or calcite becomes one of the sources of Calcium in the formation of C-(A)-S-H hydration products under the catalysis of Na_2CO_3 (Provis, Deventer, Krivenko 2008):

$$Slag + Na_2CO_3 \rightarrow CaCO_3 + 2Na^+ + + \text{dissolved Si} + Al$$

$$CaCO_3 + 2Na^+ \; Ca2+ \text{ (calcite, dolomite)} + \text{dissolved Si} + Al \rightarrow \text{C-(A)-S-H} + Na_2CO_3$$

Based upon these two chemical pathways, Moseson suggested an increase in Na_2CO_3 stimulates more limestone consumption for the formation of strength contributing C-(A)-S-H. He also derived mathematical models (Figure 2-6) to examine strength response in terms of varying slag, water, Na_2CO_3 and limestone contents. A 3-day strength as high as 40MPa could be achieved with high volume of limestone replacement in Na_2CO_3 activated slag. Moseson (2012) stated that these formulations, compared to PC, reduce both carbon dioxide

emissions and energy consumption by up to 97%. Despite its benefits, durability of high volume replacement in AAS is yet to be addressed.

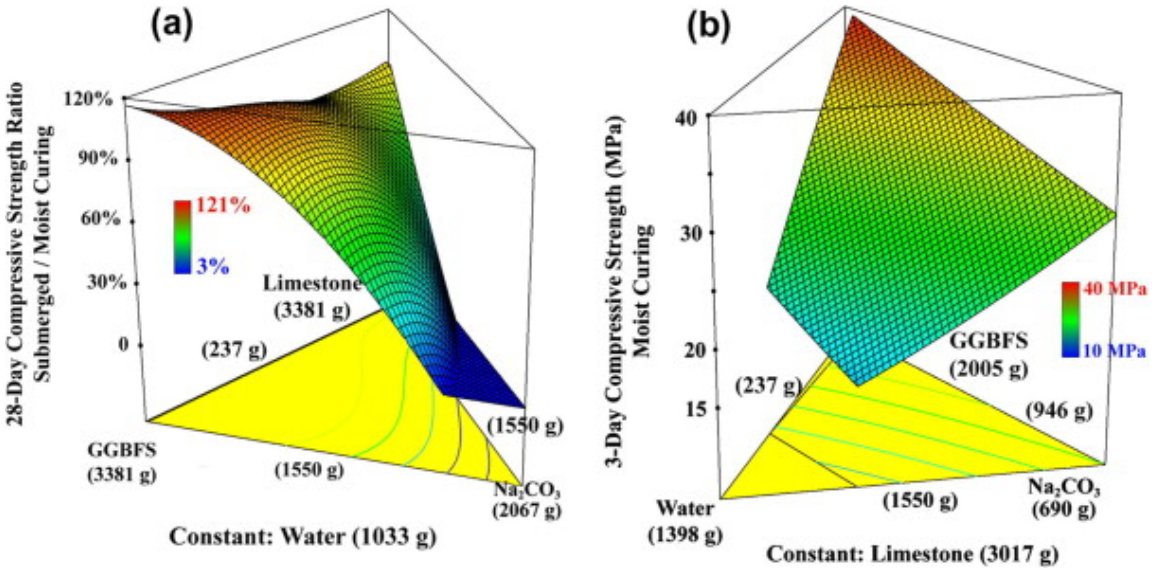

Figure 2-6 Mathematical models of achievable compressive strength with varying slag, water, Na_2CO_3 and limestone content (a) compressive strength ratio at 28day and 3day (b) compressive strength at 3day (Moseson 2012)

2.5 Magnesium oxide

Magnesium is the eighth most abundant element on Earth. Magnesium oxide (MgO) is produced from the incineration of magnesium carbonate ($MgCO_3$) or magnesium hydroxide ($Mg(OH)_2$):

$$MgCO_3 \xrightarrow{heat} MgO + CO_2$$

$$Mg(OH)_2 \xrightarrow{heat} MgO + H_2O$$

Light burned magnesia, manufactured at 700-1000°C is the most reactive magnesia with the highest surface area. It is the most expansive compared to other less reactive magnesia – dead burned magnesia and hard burned magnesia. Although the production of MgO is similar to that of lime (CaO) from limestone, a lower manufacturing temperature is required. The less energy intensive production nature has stimulated research in replacing PC with MgO (Harrison, 2008).

Reactive MgO reacts with water to form brucite ($Mg(OH)_2$): $MgO + H_2O \rightarrow Mg(OH)_2$. The formation of $Mg(OH)_2$ leads to volume expansion of ~118%. Although $Mg(OH)_2$ is expansive, the crystalline nature of $Mg(OH)_2$ is not as effective as CSH in filling large pores. An increase in pore volume and smaller pore size when MgO is added to PC leads to evidence drop in

strengths (Li 2012) and increase in drying shrinkage (Wang 2006, Yuk 2012). Yuk (2012) found that 4% addition of MgO in PC resulted in 9% increase in drying shrinkage. However, the reaction between slag and MgO is slightly different. HaHa (2011) reported porosity decreases with increase in MgO due to the high aluminium content in slag. MgO forms hydrotalcite-like phase compound, $Mg_4Al_2O_7.10H_20$ (MAH), rather than $Mg(OH)_2$. This has an improvement in homogeneity and connectivity. Nonetheless, less aluminium is incorporated in the CSH to form MAH. MAH has a lower density and a less porous structure is formed. Haha et al (2011) showed that an increase in MgO in slag led to higher compressive strengths at all ages, although the extent of impacts depended on the activators used. Limited research was performed on the influences of MgO on the shrinkage of AAS. A reduction in total pore volume is expected to reduce drying shrinkage. However, the MAH contains more chemically bonded water than the CSH. This might increase chemical and antogenous shrinkage. The impact is to be justified.

Although $Mg(OH)_2$ is less likely to form in slag, $Mg(OH)_2$ is still preferred as it is beneficial for its low soluble and mobile, relative to Portalandite ($Ca(OH)_2$), hence, more resistant to aggressive chemical attack. Brucite is also able to maintain a pH at 10.5 in the longer term while the pH of Portlandite would reduce to around 8 upon carbonation. This provides better protection for reinforcements from corrosion in the longer term.

3 Material and experimental methods

This chapter describes the materials used, mixes made and the experimental methods employed in the study.

3.1 Materials

GGBS and CEM I PC supplied by Hanson cement, limestone with particle size >150 μm provided by Tarmac and MgO, supplied by Richard Baker Harrison, with the compositions shown in Table 3-1. NaOH and Na_2CO_3, both in dry form, supplied by Fisher Scientific were used. The standard consistence (water demand) of each material was determined with a viscat apparatus according to BS EN 196-3:2005. The water-to-cement ratio of each mix was determined according to its constituents:

$$w_{total} = \sum_i p_i w_i$$

where, p = the percentage of material in each mix, w = standard consistence ratio and w_{total} = the water-to-cement ratio required

Component (% by weight)	GGBS	Limestone	MgO	PC
CaO	40.1		<1.2	65
SiO_2	36.7	< 0.2	< 3.1	20
$CaCO_3$		> 98.7		
$NaCO_3$				
Al_2O_3	10.4	< 0.2		4
MgO	7.9	0.2	> 92.0	3
SO_3	1.4			
NaOH				
Standard consistence	0.33	0.25	0.585	0.27

Table 3-1 The composition (percentage by weight) and standard consistence of GGBS, limestone, MgO and PC

3.2 Experimental methods

3.2.1 Preparation of cement samples

Due to the highly exothermic nature of the alkalis used, NaOH and Na_2CO_3 solutions were prepared from pallets/powder 24 hours before mixing to avoid lengthening of the setting time. Dry materials were weighed and poured into the mixing bowl, as seen in Figure 3-1. They were mixed dry for a couple seconds to ensure homogeneity in the powder form. Water was then poured into the mixing bowl while mixing at low speed and started timing. The mixing was stopped after 2 minutes to adhering the wall and bottom of mixing bowl, and placing the mixture in the middle with a spatula. After so, continued the mixing for another 3 minutes.

The total mixing time was 5 minutes. The mixture was then poured into moulds of different sizes.

Figure 3-1 Mixing bowl and machine for cement pastes

3.2.1.1 Cement samples for UCS and shrinkages tests

Cube moulds, 40mm x 40mm x 40mm, were used, as shown in Figure 3-2 (a) and prism moulds, 160mm x 40mm x 40mm, were used with studs fixed at the two ends of the prism for length measurement, as shown in Figure 3-2 (b). Mixture is poured into the moulds in three layers, and in between each layers the mixture is tapped with a spatula sufficiently, repeated and consistently to remove air voids through vibration.

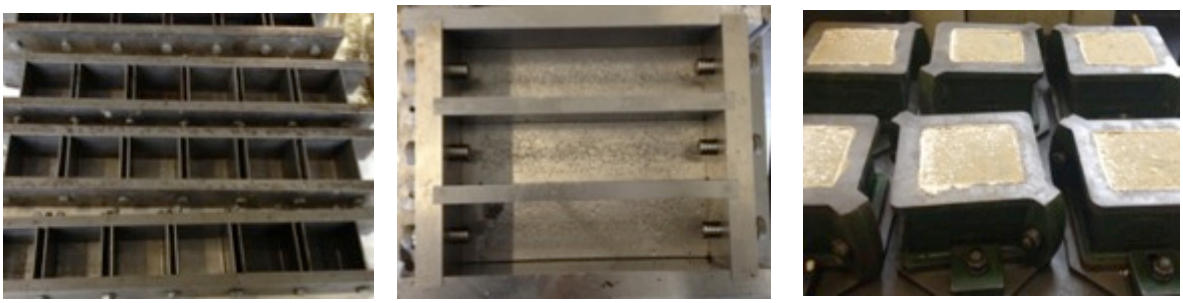

(a) (b) (c)

Figure 3-2 cement paste moulds for (a) UCS test (b) shrinkage test; (c) concrete cubes for UCS test

3.2.2 Preparation of concrete samples for UCS tests

A similar preparation method as cement pastes was used, except that a vibrating table was used rather than spatula for air voids removal. Concrete mixes were made into larger cubes of 100mm x 100mm x 100mm as shown in Figure 3-2(c). The mixes consisted of 45% coarse aggregates, 30% fine aggregates and 25% cement.

3.2.3 Curing

After 24 hours of drying at room temperature (20°C±1 °C) and humidity (51%± 3%), the samples were de-moulded. For UCS test cubes and submerged shrinkage test prisms, samples were placed in water tank until the day for tests (Figure 3-3). For drying shrinkage tests prisms, samples were exposed to the room temperature and humidity for 28 days (Figure 3-4).

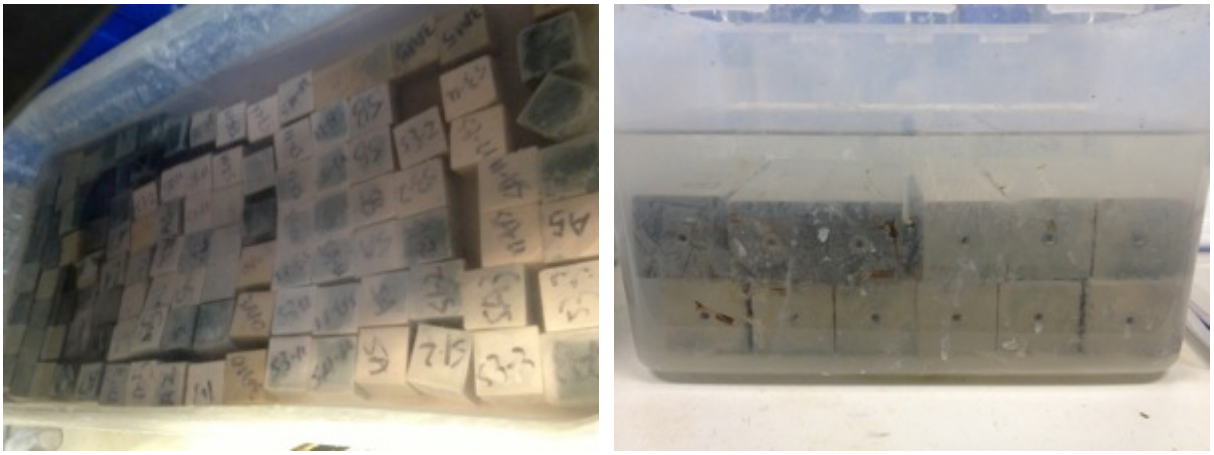

(a) (b)

Figure 3-3 The submerged samples, curing in water tank (a) UCS cement cubes (b) submerged shrinkage cement prisms

Figure 3-4 Drying shrinkage cement paste prisms at room temperature (20°C±1 °C) and humidity (51%± 3%)

3.2.1 Measurement & tests

A variety of tests were performed to examine the mechanical properties and microstructure of 28-day samples. It includes unconfined compressive strength test (UCS), shrinkage strain test, mass loss analysis, scanning electron microscopy (SEM) analysis and X-ray diffraction (XRD) analysis, electric furnace test as well as pH measurement.

3.2.2 Unconfined Compression Strength (UCS) test

UCS was determined with Control Advantest 9 machines as shown in Figure 3-4 (a) and (b). Load-controlled tests were used. Both sides of the samples were measured before the tests. Due to the difference in sizes of the cement and concrete cubes, the samples were tested with different load rates using 2400N/s and 3000 N/S respectively. Samples were tested at 4, 7 and 28 day in triplicates.

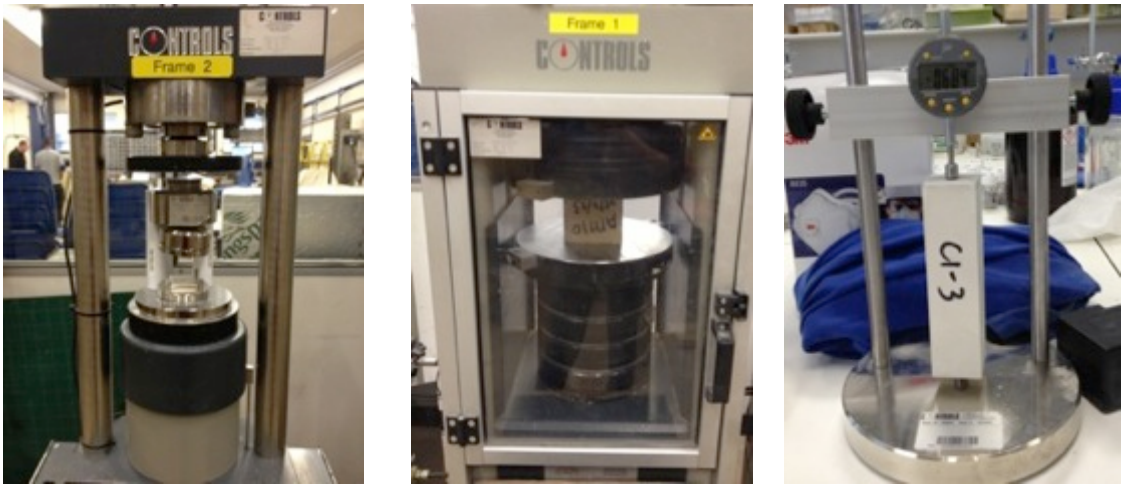

(a) (b) (c)

Figure 3-5 (a) Controls Advantest 9 machines for cement cubes (b) Controls Advantest 9 machines for concrete cubes (c) Controls length comparator

3.2.3 Shrinkage test

The shrinkage performance of cement pastes rather than concrete was examined since the introduction of aggregates in concrete reduced the drying shrinkage and there was a lack of equipment to test concrete shrinkage. The relationship between cement and concrete shrinkage can be expressed as follow:

$$\varepsilon_{concrete} = \varepsilon_{cement}(1 - A)^n$$

where A is the aggregate content and n is a constant ranges from 1.2 to 1.7 (Shi 1996). Upon de-moulding, the length of samples was measured immediately and recorded as the original lengths. Controls length comparator was used for the strain measurement (Figure 3-3(c)). The length and weight of the cement prisms were measured daily for 28 days. Length measurement tests were performed in triplicates, alongside with visual inspection. The mass loss of prisms was also considered to monitor the water evaporation or gain in hydration products. The % mass loss is calculated from [(Mn – Mo)/Mo]x100, where, Mn is mass of cubes n days after de-moulding and Mo is initial mass right after de-moulding.

3.2.4 Microstructure analysis

3.2.4.1 Samples preparation

Crushed 28-day cement paste samples were stored in acetone for at least 3 days to cease the hydration reaction. Samples were then air-dried in desiccation chamber for a minimum of 7 days to remove chemicals, and followed by heating in oven at 60°C for moisture removal. For XRD and furnace test analysis, dried samples were grounded into fine powder using pestle and mortar. The grounding process was divided into 3 stages to ensure both soft and hard samples were obtained for the analysis. The powder was then sieved to <75μm. For SEM analysis, flat samples with a diameter of 5mm obtained from the middle of the cement cubes were used.

3.2.4.2 X-Ray Diffraction (XRD)

Approximately 1g of powder samples were pressed into an aluminium plate with a 20mm x 15mm x 2mm hole and was placed into the loading arm of Siemens D500 X-ray diffraction system to obtain the XRD patterns, as shown in Figure 3-6(a). This system uses copper anode x-ray tube with minimum 70% intensity to emit radiation. Intensity and diffraction angle of the diffracted x-ray was measured. Table 3-2 shows the parameters for the analysis.

From	To	Steps/2 sec	Step size
5	60	0.06	0.05

Table 3-2 XRD analysis parameters

3.2.4.3 Scanned electron microscope (SEM)

The JOEL model JSM-820 was used for SEM analysis as shown in Figure 3-6(b). Flat samples were mounted to metal stubs with carbon tapes and coated with gold film to produce high-resolution images via conduction. During the examination, samples were placed into the vacuum chamber. Micrographs with magnifications x500, x1000, x2500 and x5000 were obtained.

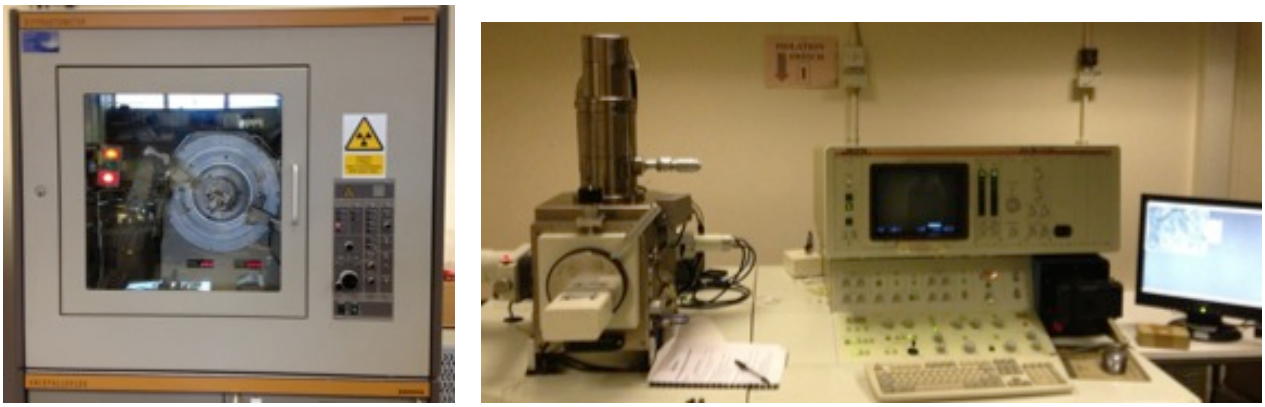

(a) (b)

Figure 3-6 (a) XRD machine; (b) SEM machine

3.2.4.4 Furnace test

Furnace test was used to determine the relative content of CSH by removing chemically bonded water molecules. The fine powder samples were placed in the 100°C oven for one day to remove moisture trapped. 1g samples were transferred into furnace (Figure 3-6(a)) and left at 300°C for 2 hours to enable complete removal of water from CSH. The change in weight after the furnace test gives an indication of the relative content of CSH present. Samples were tested in duplicates.

3.2.5 pH measurement

Due to GGBS high sensitivity to pH, pH of mixes slurry, with w/c=10:1, was measured with a EUTECH pH510 machines, with an accuracy of 0.01. The machine is calibrated with pH 4 and pH 7 solutions prior to each measurement. Samples were tested on the 1st, 4th, 7th, 18th and 28th day in duplicates.

(a) (b)

Figure 3-7 (a) Electric furnace; (b) EUTECH pH510 machine

3.3 Experimental design - Mix details

3.3.1 Overview

The experimental work began with testing the cement pastes to obtain the more pronounced effect of the change in composition proportions as well as activators contents. The cement paste tests were categorized into three main sets as below. 28-day shrinkage tests were performed on selected mixes due to the limited equipment available. Cement pastes with highest UCS were chosen and made into concrete to determine the UCS in concrete.

3.3.1.1 Test set 1

Aim: Investigate the effect of the increasing limestone content with 5% Na_2CO_3 activators. Moseson (2012) results showed that mixes composed of 50% slag, 50% limestone and 5% Na_2CO_3 yielded a 28-day compressive strength of 41.6MPa, yet, shrinkage performance and microstructure were not addressed. Mixes with slag activated by 5% Na_2CO_3 only acts as the control in this test set. C1, S-L20 and S-L50 were selected for the shrinkage tests. Composition of mixes detailed as below.

3.3.1.2 Test set 2

Aim: Investigate the effect of the varying combinations and dosages of activators on slag and limestone mix.

GGBS and limestone mixes activated by NaOH was examined to determine the effect of chemical reaction between $CaCO_3$ and NaOH on both strength and shrinkage. A combination of the two alkali activators was also used. Since Moseson (2012) suggested that Na_2CO_3 stimulates the consumption of Ca in limestone to form C-(A)-S-H, an increase in Na_2CO_3 dosage was also examined. To ensure sufficient limestone for this process, the effect of Na_2CO_3 was tested on mixes with both 80% and 50% slag.

3.3.1.3 Test set 3

Aim: Investigate the effect of small variation of MgO in slag and limestone mixes. The formation of $Mg(OH)_2$, M-S-H and M-A-H are both strength contribution and shrinkage restraining.

3.3.2 Cement and concrete mix compositions

The cement paste compositions by percentage weight are shown in Table 3-3 grouped according to test set. The percentage of slag and limestone adds to 100 and those of the activators and MgO are included as additives. Replacement levels of limestone of up to 50% were used. The activators were used in percentage weight addition of up to 15%, although most were 5%. When both NaOH and Na_2CO_3 were used, the ratio was 1.5:3.5. The w/c ratios are as calculated above from the standard consistence of the individual components, as discussed in section 3.1. A benchmark PC-Slag mix with 1:1 ratio at a w/c ratio of 0.3 for shrinkage testing was denoted B. Concrete mixes were made for the slag:limestone ratio of 4:1 with the w/c ratios, activator and aggregates contents as shown in Table 3-5. 20kg of concrete was made for each mix.

Set	Description	Code	w/c	GGBS	L	Na_2CO_3	NaOH	MgO
1	Change in slag to limestone ratio (at 5% Na_2CO_3)	C1#	0.33	100		5		
		S-L20#	0.3	80	20	5		
		S-L30	0.29	70	30	5		
		S-L40	0.29	60	40	5		
		S-L50#	0.29	50	50	5		
2	Change in slag to limestone ratio (at 5% NaOH)	C2	0.33	100			5	
		NH5#	0.31	80	20		5	
		S-L50N	0.29	50	50		5	
	Replacement of Na_2CO_3 by NaOH	S-L20#	0.3	80	20	5		
		NH1.5#	0.31	80	20	3.5	1.5	
		NH5#	0.3	80	20		5	
	Increase in Na_2CO_3 dosage (80% GGBS)	NC2.5	0.3	80	20	2.5		
		S-L20#	0.3	80	20	5		
		NC10	0.31	80	15	10		
		NC15	0.32	80	10	15		
	Increase in Na_2CO_3 dosage (50% GGBS)	S-L50#	0.29	50	50	5		
		3NC10	0.27	50	45	10		
		3NC15	0.26	50	40	15		
3	Addition of MgO on 5% Na_2CO_3 activated slag (80% GGBS)	S-L20#	0.3	80	20	5		
		M5	0.33	80	15	5		5
		M10	0.34	80	10	5		10
	Addition of MgO on 5% Na_2CO_3 activated slag (50% GGBS)	S-L50#	0.29	50	50	5		
		3M5	0.30	50	45	5		5
		3M10	0.32	50	40	5		10
		3M15	0.34	50	35	5		15
		3M20	0.36	50	30	5		20
	Addition of MgO on 1.5%NaOH+3.5% Na_2CO_3 activated slag (80% GGBS)	NH1.5#	0.31	80	20	3.5	1.5	
		AM5	0.32	80	15	3.5	1.5	5
		AM10#	0.34	80	10	3.5	1.5	10

Table 3-3 Cement mixes detail (%by weight on basis of 105)

Code	w/c	GGBS	L	Na_2CO_3	NaOH	MgO
S-L20	0.30	80	20	5		
NH1.5	0.31	80	20	3.5	1.5	
AM10	0.34	80	10	3.5	1.5	10

Table 3-4 Selected cement mix to be made into concrete (%by weight on basis of 105)

Concrete mixCode	w/c	GGBS	L	Na_2CO_3	NaOH	MgO	Coarse aggregates	Fine aggregates
S-L20	1.50	3.81	0.95	0.24			8	7
NH1.5	1.55	3.81	0.95	0.17	0.07		8	7
AM10	1.70	3.81	0.48	0.17	0.07	0.48	8	7

Table 3-5 concrete mix details (in kg)

4 Results & Discussions

This section details the results from UCS test, strain measurement in both dry and wet curing conditions, and microstructure analysis of cement mixes composed of slag, limestone and Magnesium oxide that are activated by different combination or dosage of alkalis as specified in the previous chapter.

4.1 Investigation on cement paste

4.1.1 Test set 1: Varying slag to limestone ratios with 5% Na_2CO_3 activators

4.1.1.1 Strength performance

This first set of cement mixes consisted of slag and limestone activated by 5% of Na_2CO_3. A range of slag to limestone ratios, 100/0(C1), 80/20(S-L20), 70/30(S-L30), 60/40(S-L40) and 50/50(S-L50), were examined. Figure 4-1 shows the effect of limestone on the 4, 7 and 28-day UCS. As seen from Figure 4-1, there is an evident reduction in compressive strength with the increase in limestone content. The UCS values drop from 50.6 MPa to 37.0 MPa when the 50% of slag was replaced by limestone. Although the UCS for GGBS:Limestone = 50/50 obtained was slightly lower than Moseson (2012) reported value - 41.6MPa, it was considered to be in agreement as GGBS used by Moseson contained 4% more of SiO_2 and Al_2O_3 in total. Since Ca can be obtained from limestone, more strength contributing CSH and CAH was formed in Moseson's mix.

Mixes with only 20% replacement of GGBS by limestone had a significantly lower early strength than C1, but the two mixes yielded a similar 28-day UCS at ~50 MPa. The low early strengths might be due to the drop in blend pH as GGBS was replaced, hence, a lower hydration rate, as shown in Figure 4-2. At late stage, the effect of the pH became insignificant. Instead, a similar 28-day strength showed that strength gain attributed from the denser structure attained by 20% limestone filler was sufficient to compensate the loss in strength due to the 20% reduction in GGBS. However, as the limestone content increased to 50%, the strengths at all ages dropped as dilution effect of GGBS overrides the filling effect.

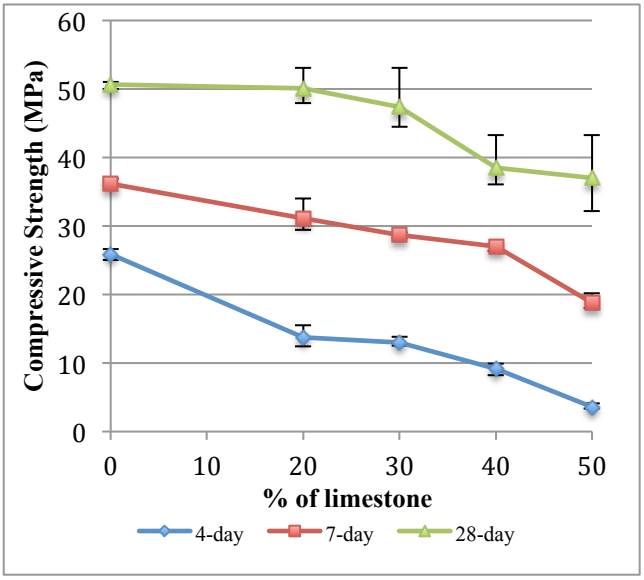

Figure 4-1 UCS of 5% Na_2CO_3 activated slag pastes as S:L ratio varied

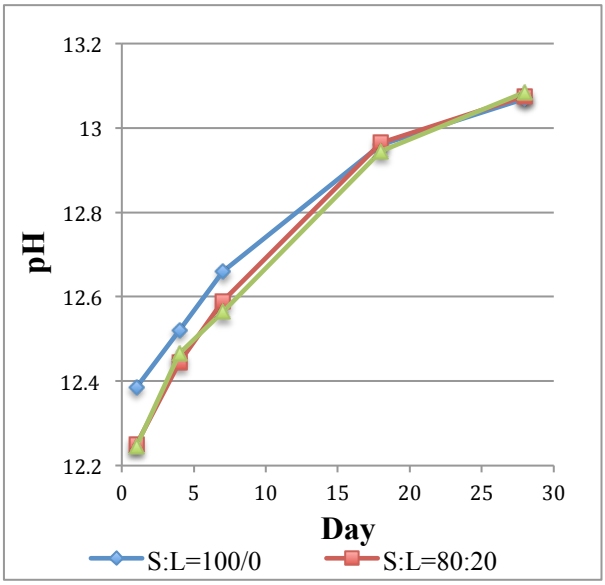

Figure 4-2 pH of 5% Na_2CO_3 activated slag paste as the S:L ratio varied

4.1.1.2 Drying shrinkage performance

Free drying shrinkage strain tests alone do not provide extensive information on concrete behaviour since all concretes are restrained in different ways, either by reinforcement or structure. However, drying shrinkage tests can offer the relevant information on how the shrinkage stresses develop. Prisms length was measured by gauge meter with an accuracy up to 0.001mm, and performed in triplicates. The margin of error determined was up to $\pm$0.03% change in length. The shrinkage performance was compared against a commercial blend of cement paste (CEM III) (B). Its 1-day and 28-day drying shrinkage were -0.04% and -0.23% respectively.

Figure 4-5 shows the strain development for cement paste with S:L = 100/0(C1), 80/20(S-L20) and 50/50(S-L50). It was observed that an increase in limestone content resulted in higher shrinkage. S-L50 28-day strain was 63.5% higher than that of C1. The effect of limestone in AAS was similar to that in PC. It might be due to the resulting less porous structure. Pipilikaki (2009) reported that the addition of limestone up to 35% in PC reduced the threshold diameter of the paste. Threshold diameter represents the minimum diameter that is geometrically continuous throughout the hydrated cement paste. This behaviour can be attributed to the better packing of particles due to the filling effect of the limestone powder. Assuming limestone has similar effect in AAS, the smaller the pore size results in a larger capillary tensile forces set up at the meniscus, hence, higher shrinkage.

Weight change was also considered in the study, as it represents the evaporation of free water. 24 hours after de-moulding, C1, S-L20 and S-L50 had 2.0%, 5.0% and 5.2% reduction in

weight respectively(Figure 4-6). The significant water loss within 24 hours explained the severe surface cracking observed from day 1 after de-moulding(Figure 4-3). Upon 28-day of drying, weight loss of mixes with 50%(S-L50), 20%(S-L20) and 0%(C1) of limestone were 18%, 12% and 8% respectively. Figure 4-4 suggests tight correlation between the water loss and drying shrinkage on 28-day. This suggests rapid water evaporation led to the lack of water for hydration to fill the voids and an increase in total pore volume for shrinkage. Since nearly 70% of weight loss occurred within the first 7 days of drying for all mixes, degree of initial hydration is critical in improving shrinkage performance. Antogenous shrinkage is the other possible cause of increase in shrinkage, since the w/c ratio decreases as limestone content increases. S-L50 might have high autogenous shrinkage.

Drying shrinkage of C1 was 1.8 times higher than B, while similar weight loss was observed. The main cause of high shrinkage was the lack of crystalline compounds and expansive ettringite slag and limestone mix to restrain collapse of CSH or compensate shrinkage. This reaffirms the need of crystalline and expansive products.

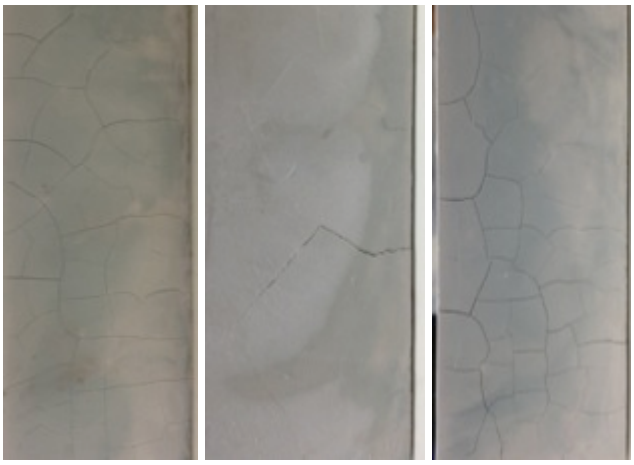

(a) (b) (c)

Figure 4-3 Surface cracking on 1-day (a) C1 (b) S-L20 (c) S3 S-L50

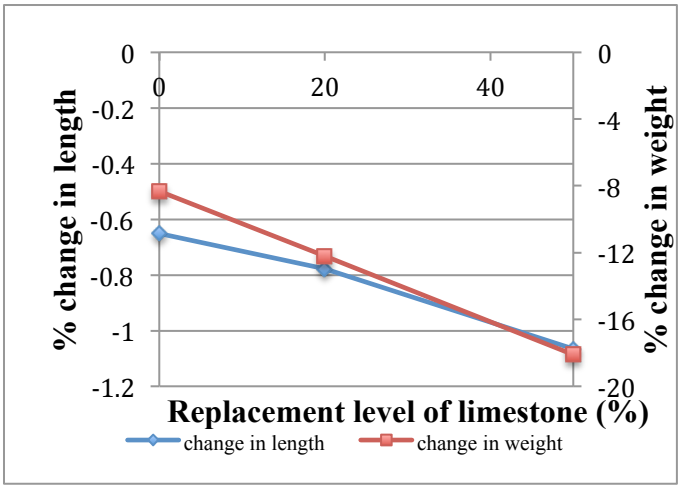

Figure 4-4 Relationship between limestone content and drying shrinkage on 28-day

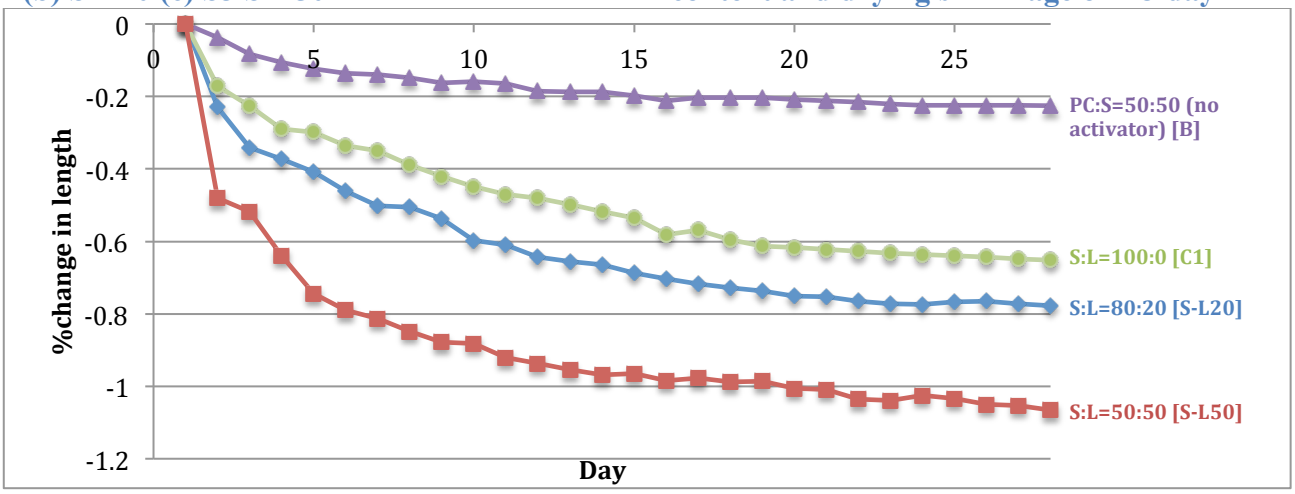

Figure 4-5 Drying strain development of 5% Na_2CO_3 activated with S:L varied

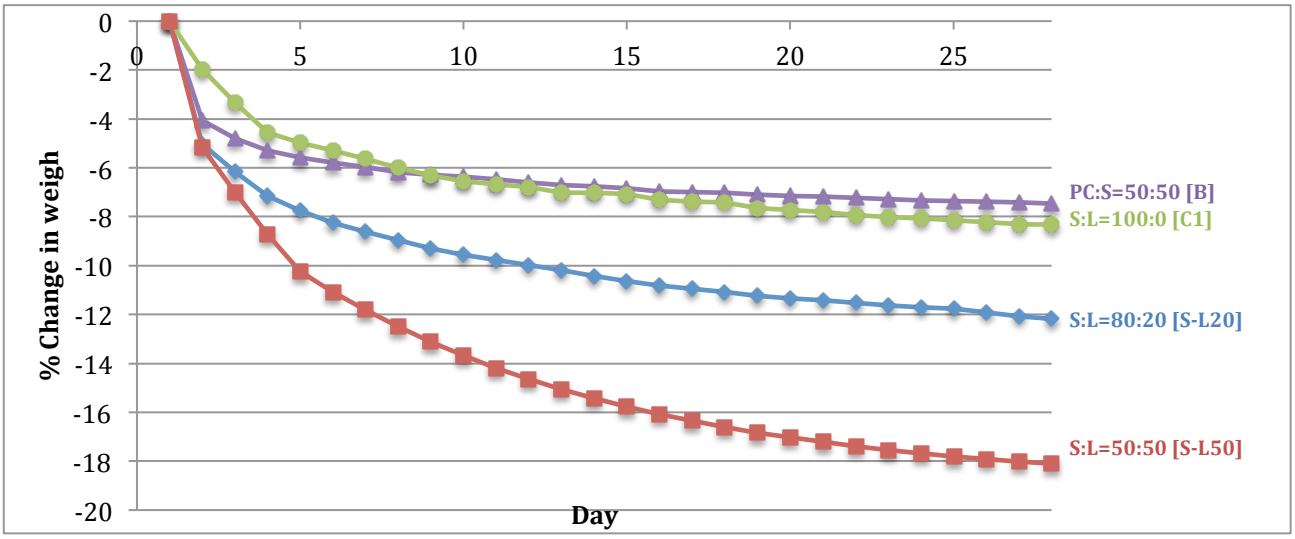

Figure 4-6 Drying weight loss of 5% Na_2CO_3 activated with S:L varied

4.1.1.3 Submerged shrinkage performance

In construction, cement and concrete are kept wet during curing, therefore, shrinkage performance in submerged condition was also assessed. Figure 4-7 shows the strain development of pastes cured in water (NOTE: different y-axis scale in Figure 4-5 and 4-7). The 28-day strain attained in wet condition was $1/10^{th}$ of that in dry, due to the uptake of external water for the hydration process and prevented collapse of CSH. However, shrinkage was observed rather than typical expansion of ordinary PC. This might be due to the high chemical and autogenous shrinkages (Fang et al 2011), as well as rapid water evaporation. Localised drying of internal pores led to shrinkage and it took time for the water restoration and consequential hydration to fill voids and cracks. As a result, shrinkage did not cease until 2-4 days after submerging. The restoring of length generally began after 14 days of water-curing. The rate of expansion increases with the limestone content. This might be due to the denser distribution of cracks and voids formed in S-L50 over 24hours of hardening. This increases in surface area for the hydration of expansive CSH, hence, higher expansion rate. The dense distribution of microcracks in S-L50 were evidence of expansion. In contrast, mixes with PC:GGBS=1:1 (B) almost had no shrinkage or expansion over 28-days, as PC hydration products has similar volume as its initial compounds. This work shows the importance of maintaining a humid environment during hardening as well as the initial hydration rate improvement to limit water evaporation.

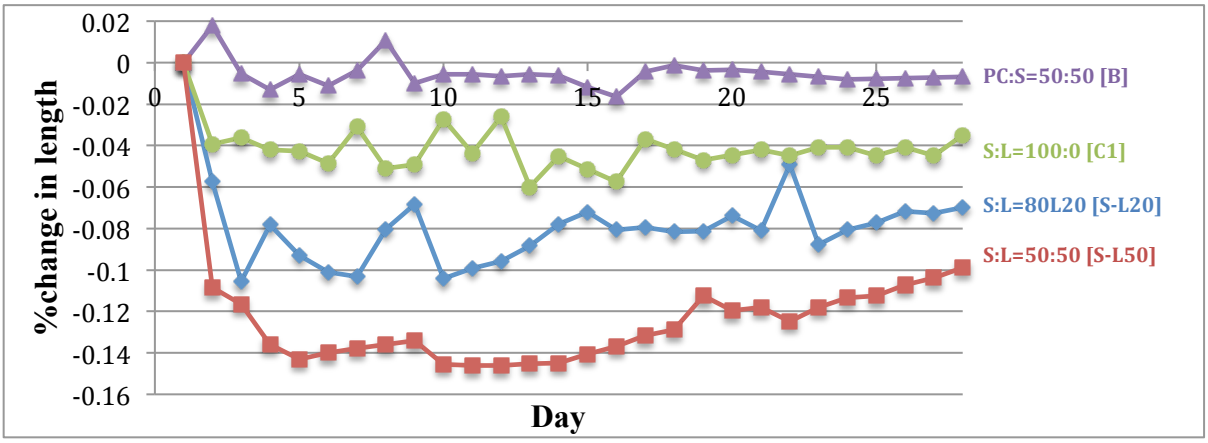

Figure 4-7 Submerged strain development of 5% Na_2CO_3 activated with S:L varied

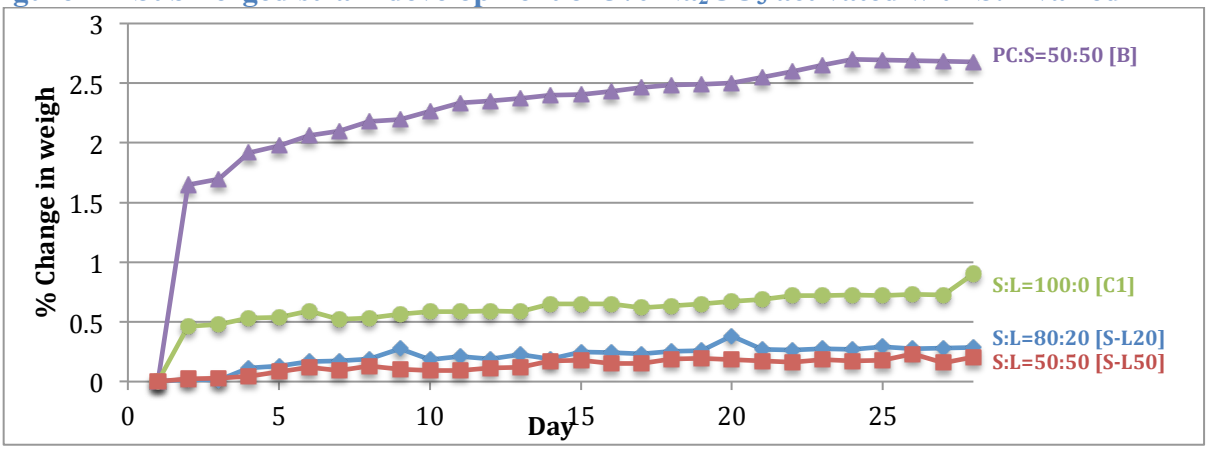

Figure 4-8 Submerged weight loss of 5% Na_2CO_3 activated with S:L varied

4.1.1.4 Microstructure analysis

Upon calcination at 300°C for 2 hours, mixes with 0% (C1), 20% (S-L20) and 50% (S-L50) limestone had 5.47%, 3.90% and 2.34% drop in weight respectively. Since the chemical formulas of CSH vary, the exact CSH amount cannot be determined but there was an evidence reduction in CSH resulted from the dilution of slag. S-L20 and S-L50 were also examined with XRD (Figure 4-9). However, $CaCO_3$ and CSH share the same peaks in the XRD analysis. It is impossible to tell if the C-(A)-S-H was formed from the Ca in limestone. Considering the peak at 29°, the intensity of S-L50 is more than double of that with 20% limestone, while S-L50 contained less CSH as indicated by furnace test, it implied that large portion of limestone remained unreacted, and simply acted as insert filler in S-L50.

SEM analysis was performed on S-L20 and S-L50 (Figures 4-10 and 4-11respectively). Both S-L20 and S-L50 samples displayed uniform and dense distribution of CSH gel. This might due to the limestone filling effect. However, S-L50 shows a significantly denser distribution of microcracks than S-L20. The surface of S-L50 also appeared to be looser due to the presence of excessive unreacted limestone. This suggests that the excessive presence of limestone reduces the homogenousity and connectivity of C-S-H, hence lower strength.

Figure 4-12 shows the micrographs of B, no microcraks can be identified and needle-like expansive ettringite could be seen. This explained its drying shrinkage performance.

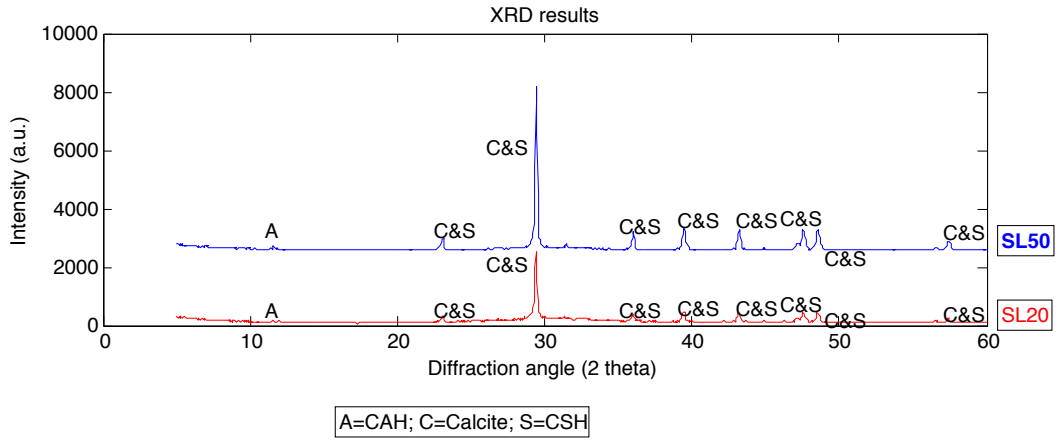

Figure 4-9 XRD analysis of S-L20 and S-L50

With only 20% of limestone replacement, a 28-day compressive strength compatible to that without limestone was achieved, yet, this led to an increase in 28-day strain in both dry and wet condition by 19% and 99% respectively. More importantly, the shrinkage performance of 5% Na_2CO_3 activated slag and limestone mixes had a shrinkage performance several magnitude higher than the commercial cement blend B. Severe surface cracking was also observed.

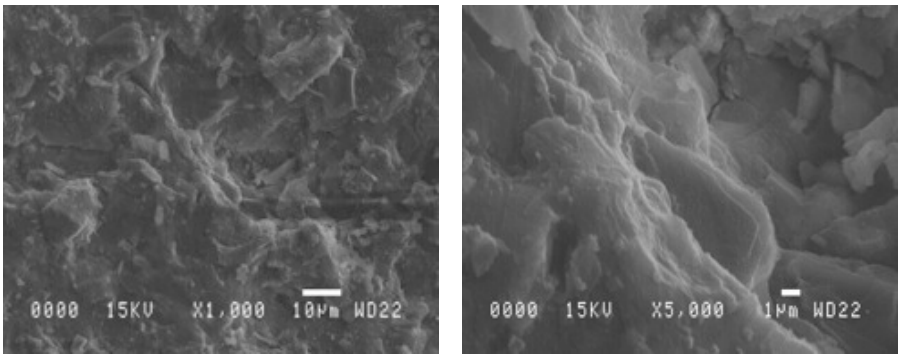

(a) (b)

Figure 4-10 Microscopic photo of S-L20 (a) x 1000 (b) x5000

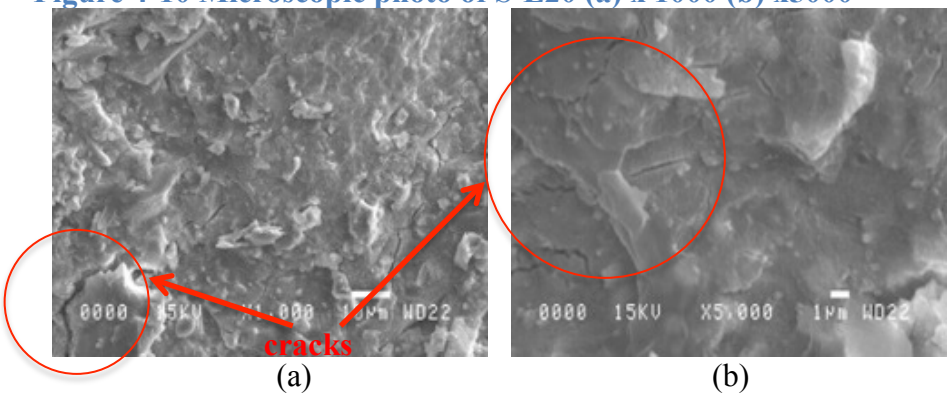

(a) (b)

Figure 4-11 Microscopic photo of S-L50 (a) x 1000 (b) x5000

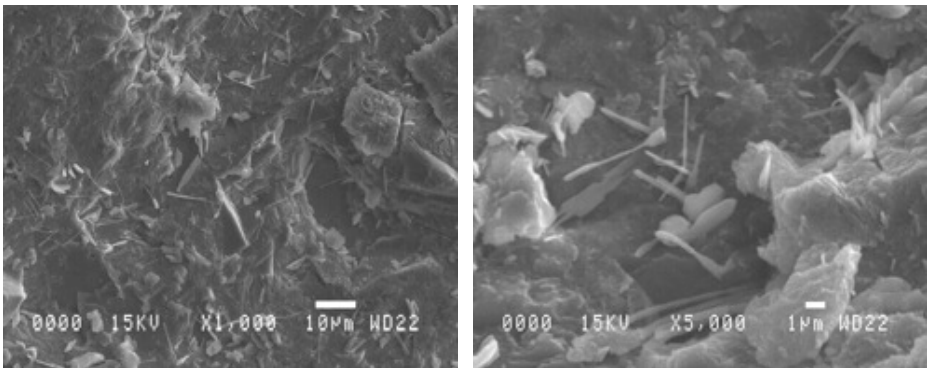

(a) (b)

Figure 4-12 Microscopic photo of B (a) x 1000 (b) x5000

4.1.2 The effect of change in activators content

The second set of experiments focused on the effect of activators on mixes with 80% of slag and the remaining as limeston, since NaOH can improve early strength as well reacting with $CaCO_3$.to form crystalline $Ca(OH)_2$. The effect of replacing Na_2CO_3 by NaOH was examined on mixes using 5% NaOH (NH5) and 1.5% NaOH with 3.5% Na_2CO_3 (NH1.5).

4.1.2.1 With 5% NaOH activator

Strength performance

Figure 4-13 shows the use of NaOH activator offered a higher 4-day UCS due to the higher initial pH attained at ~13.2 at all ages irrespective to the slag to limestone ratios. The 28-day UCS of NaOH activated slag were lower, due to the lack of Na_2CO_3 to catalyse the consumption of Ca from limestone for the formation of C-(A)-S-H as well as a more porous structure formed as discussed in section 2.3. The most important finding in this test set was the difference in strength reduction upon 50% slag replacement by limestone with difference activators. The strengths drop for 5% NaOH activated slag and 5% Na_2CO_3 activated slag were 18.5% and 26.9% respectively. There are two possible causes. First, strength contributing $Ca(OH)_2$ were formed from the reaction between NaOH and limestone. Second, NaOH activated slag had more porous structure than Na_2CO_3 activated slag. The addition of limestone had a more pronounced filling effect on NaOH activated mixes. The denser structure upon limestone addition led to less reduction in strength as limestone was added. However, neither XRD nor SEM analyses could identify which effect is more dominating.

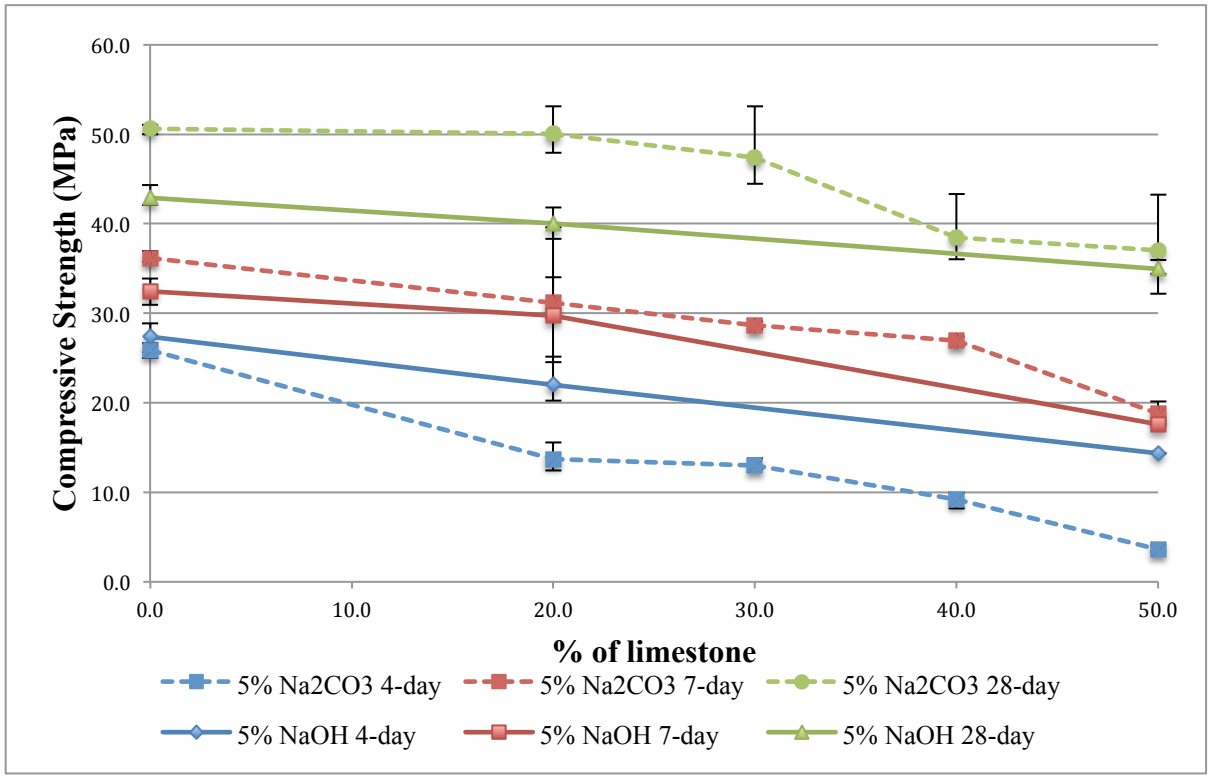

Figure 4-13 UCS of slag paste activated by different activators at 5% Na_2O dosage, S:L varied

4.1.2.2 Partially replacing Na_2CO_3 by NaOH

Strength performance

Although $Ca(OH)_2$ is formed under the presence of NaOH, the strength contributed by $Ca(OH)_2$ was insufficient to compensate the drop in strength resulted from the porous structure developed from NaOH activated slag. Given a drop in 28-day strength, slag activated by a combination of NaOH and Na_2CO_3 was tested.

Figure 4-14 shows that with only 1.5% replacement of Na_2CO_3 by NaOH, UCS increased at all ages. The 4-day and 28-day strength increased by 24% to 30.7 MPa and 6% to 53 MPa respectively. This result agreed with Li and Sun (2000) and Collins and Sanjayan (1998) reports on a combination of NaOH and Na_2CO_3 yielding an early strengths higher than that activated by NaOH and Na_2CO_3 alone. Meanwhile, $Ca(OH)_2$ was also formed. By maintaining a certain portion of Na_2CO_3, Ca was consumed from limestone to form C-(A)-S-H occurred, as well as relatively dense structure, hence, a high 28-day strength.

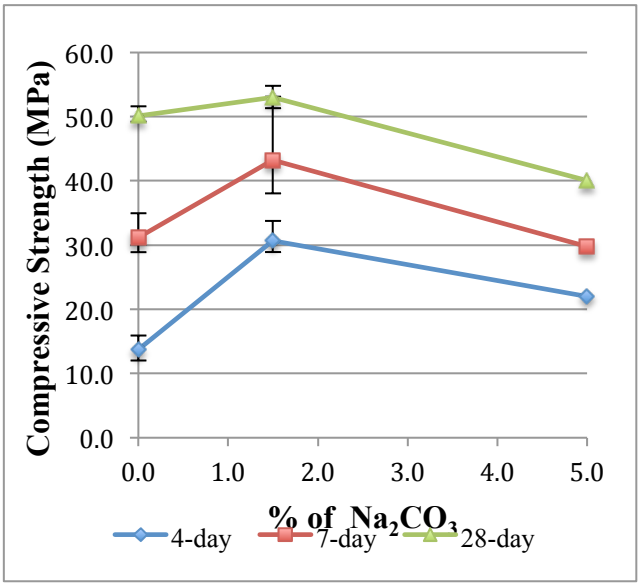

Figure 4-14 UCS of Na_2CO_3 and NaOH combination activated slag paste (80%GGBS, 5%Na_2O)

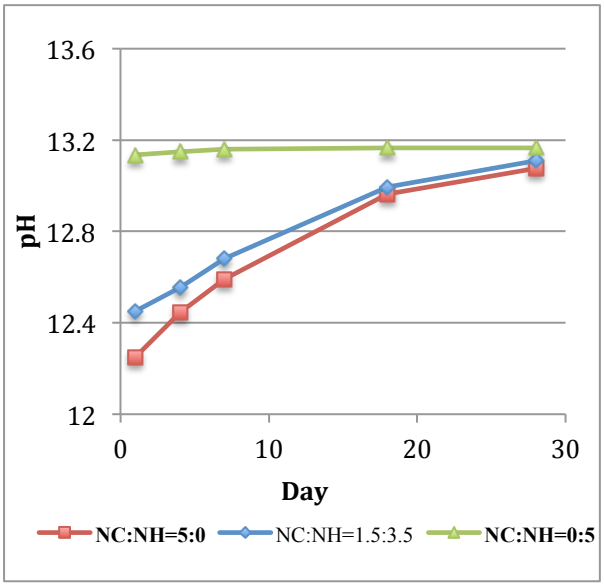

Figure 4-15 Change in the pH of Na_2CO_3 and NaOH combination activated slag paste (80%GGBS, 5%Na_2O)

Drying shrinkage performance

Laboratory studies showed the shrinkage performance is highly dependent on the nature and dosage of activators used. As reported by Collin and Sanjayan (2001), alkali-activated 100% slag in drying condition has serious surface cracking irrespective to the activator types. However, Figure 4-16 (b) of NH5 displayed no surface cracks at all over 28days of drying. This was a very important finding, as this suggested limestone played a critical role in restraining the shrinkage under the presence of NaOH, as crystalline phase $Ca(OH)_2$ was formed As water evaporated from the paste during shrinkage, CSH collapsed while $Ca(OH)_2$ remained unaffected, hence, $Ca(OH)_2$ restrainted the CSH shrinkage. The presence of $Ca(OH)_2$ was proved by the microstructure analysis.

Although no strain tests were performed on mixes with 100% slag activated with 5%NaOH activated slag., Shi (1996) showed that the strain developed from drying shrinkage of Na_2CO_3 and NaOH activated slags had a ratio of 93:111 at 231 days. Cincotto (2007) also found that the shrinkage of 5% NaOH activated slag was at ~0.6% strain at 28 days. It is therefore reasonable to assume that 28-day drying shrinkage of 5% NaOH activated slag only cement paste lies between 0.35% and 0.6%, and this is higher than the measured 0.18% 28-day strain of NH5 (Figure 4-17). This gave further evidence that a 20% addition of limestone with the presence of NaOH reduces shrinkage

Nonethless, NH5 had less drying shrinkage than the commercial CEM III blend mix B, even though NH5 had much less weight loss than B over the 28-days of drying. Again, this showed the importance to improve pore structure for better shrinkage performance.

Figure 4-17 shows the strain development over 28 days. After 24 hours of de-moudling, the length contraction of NH1.5 and NH5 were 1/10th and 1/4th of that of S-L20, while there were 47% and 76% reduction in 28-day strain for NH1.5 and NH5 respectively. The improvement might also be due to the higher hydration rate at early stage that enabled sufficiently rapid consumption of free water and filled the voids. Less mesopores reduces spaces for shrinkage and cracking. Figure 4-18 showed the evident reduction in water loss as Na_2CO_3 was replaced by NaOH. In additional, as reported by Shi (1996), the coarser capillary pore structure of NaOH activated slag also limited shrinkage, as less capillary tensile forces in meniscus resulted.

(a) (b)

Figure 4-16 Surface cracking on 1-day (a) with NC:NH=3.5:1.5 (fine crcaks) (c) with NC:NH=0:5 (no cracking)

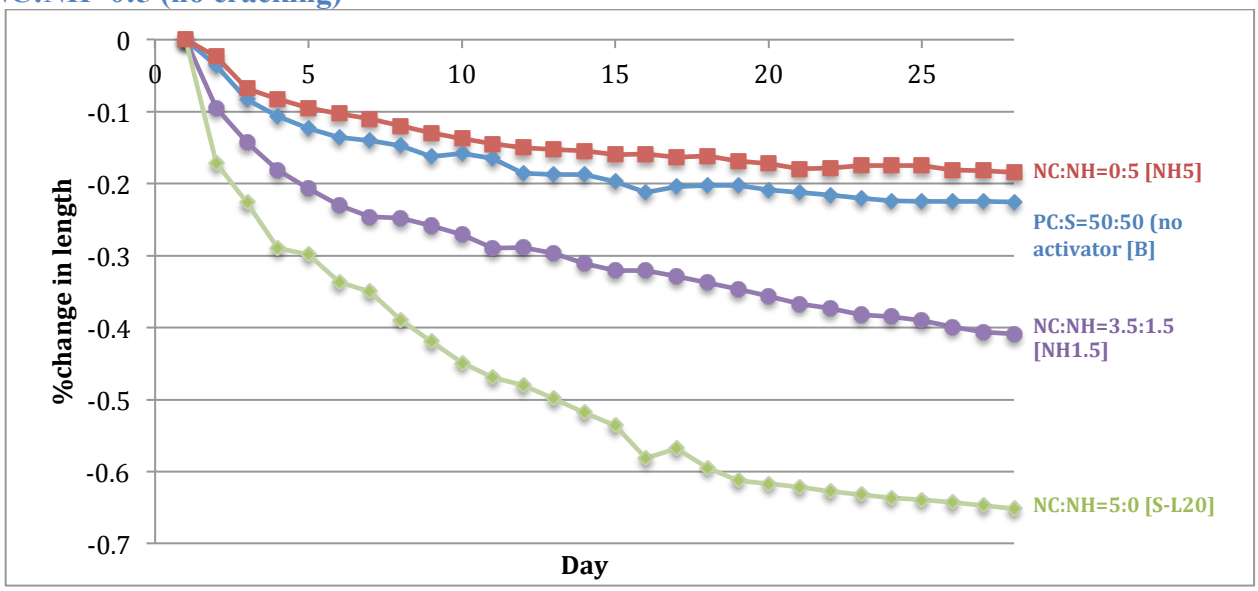

Figure 4-17 Drying strain development 5% Na_2O activated slag past at S:L=80/20, activators composition varied

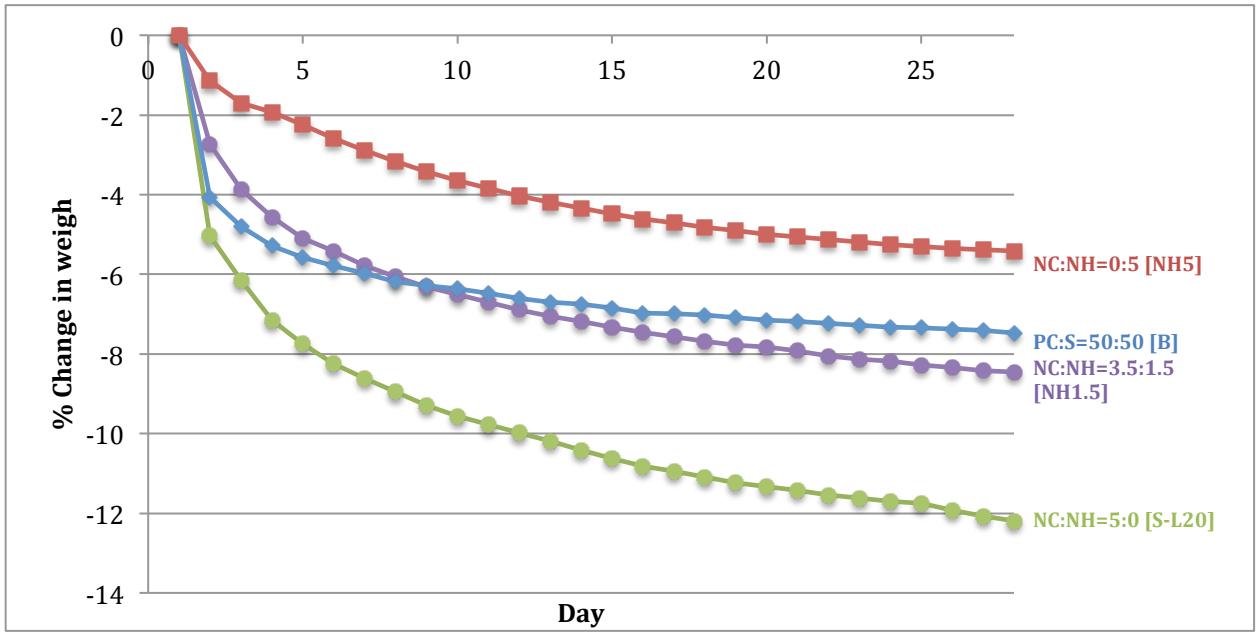

Figure 4-18 Drying weight loss 5% Na_2O activated slag past at S:L=80/20, activators composition varied

Submerged shrinkage performance

In wet condition, mixes with GGBS:limestone = 80:20 had ~0.07% reduction in length at 28 day irrespective to the activators used (Figure 4-19), as external water was available to prevent CSH shrinkage and for the hydration of GGBS. However, (NH1.5) mixes had a slightly higher gain in weight (Figure 4-20) and suggested the uptake of more water to form CSH. This explains the higher UCS of NH1.5.

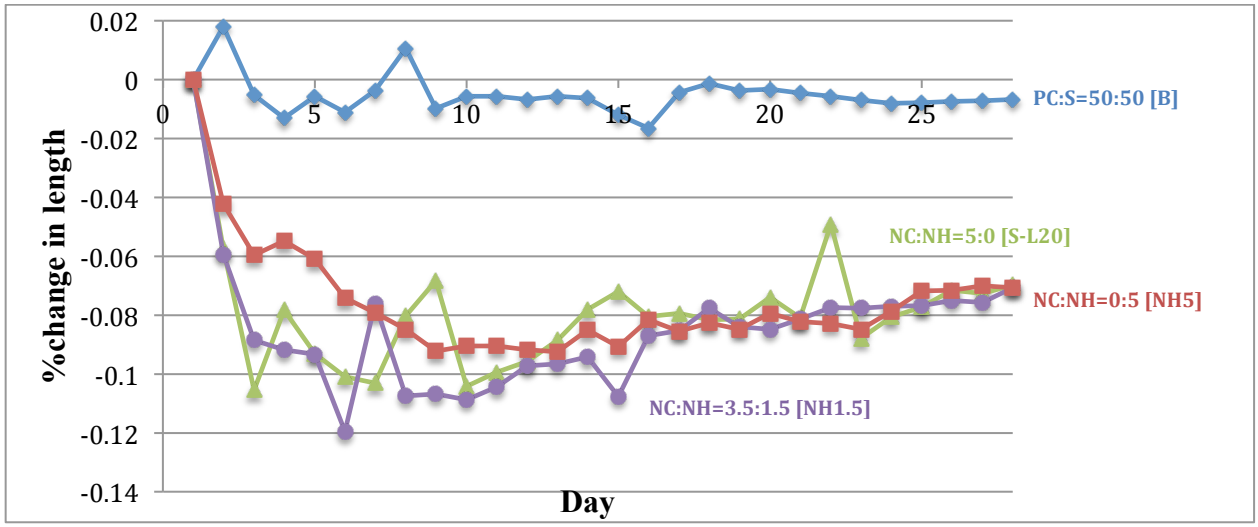

Figure 4-19 Submerged strain development 5% Na_2O activated slag past at S:L=80/20, activators composition varied

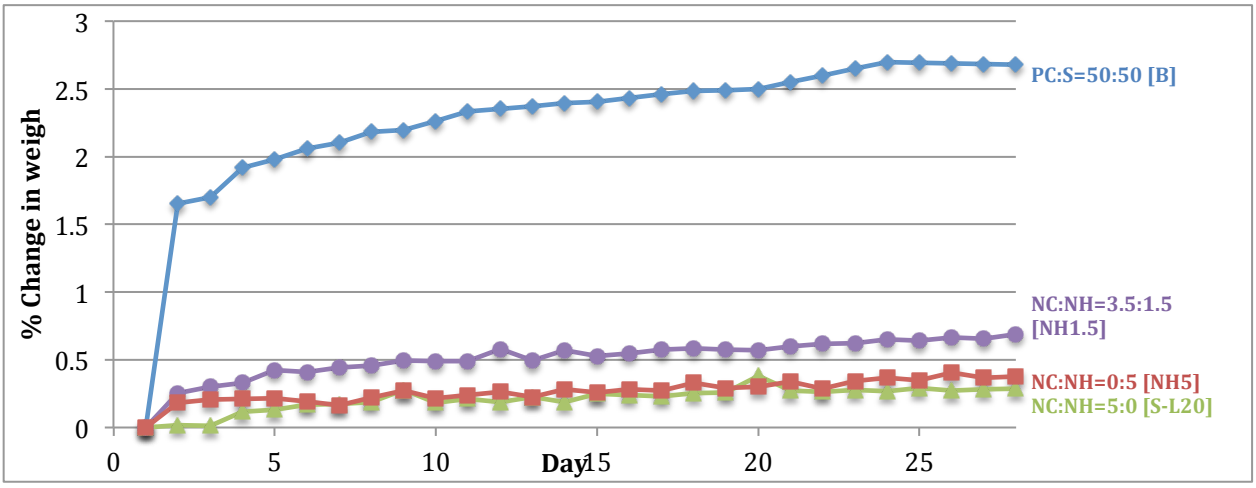

Figure 4-20 Submerged weight loss 5% Na_2O activated slag past at S:L=80/20, activators composition varied

Microstructure analysis

SEM analysis was performed on NH1.5 (Figure 4-22). Microcracks can still be found, yet, at a much lower density. The hexagonal plates were evidence of $Ca(OH)_2$ decomposed from the limestone in the presence of NaOH. However, from the XRD results in Figure 4-21, no peaks of $Ca(OH)_2$ were identified. This suggested <0.5% of $Ca(OH)_2$ presence. The addition of NaOH led to a higher and border peak at 11°. This was in agreement with Shi and Day (1996) that more CAH hydration products are formed in NaOH activated slag. Although no SEM analysis was performed on NH5, it was believed that a higher percentage of crystalline $Ca(OH)_2$ and CAH would be found.

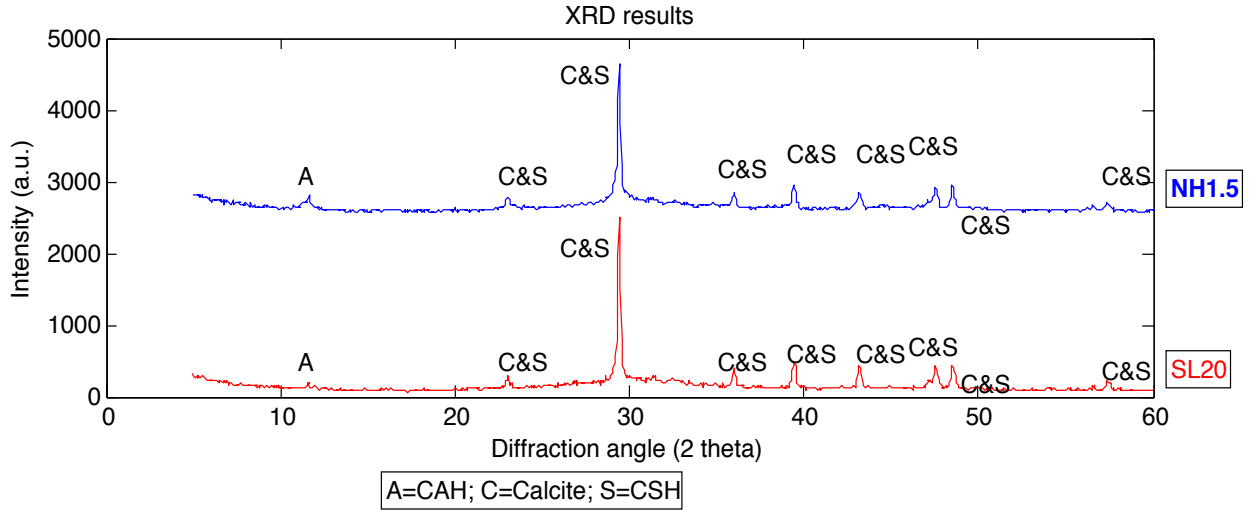

Figure 4-21 XRD results of NH1.5 and S-L20

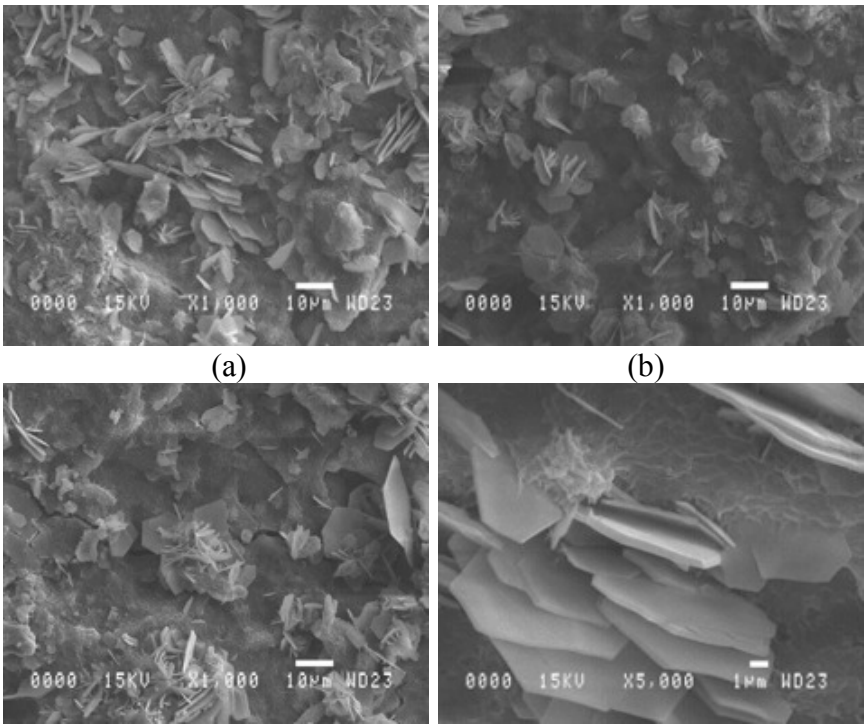

(a) (b)

(c) (d)

Figure 4-22 SEM analysis of NH1.5 (a) x1000 (b) x1000 (c) x1000 (d) x5000

4.1.2.3 Increasing Na_2CO_3 dosage

Strength performance (80% GGBS)

As suggested by Moseson (2012), Na_2CO_3 catalyses the limestone consumption to form C-(A)-S-H. Based on this assumption, UCS should increase with Na_2CO_3 dosage. Figures 4-23 shows the UCS results as Na_2CO_3 dosage increased from 2.5% to 15%. The 4-day early UCS increased as the Na_2CO_3 content increased from 2.5% to 10%, due to the higher pH attained. However, as the dosage of Na_2CO_3 continued to increase, UCS dropped. This might due to the retardation effect of Na_2CO_3 and the formation of gaylussite and thermonatrite as discussed in section 2.3. This retardation effect became more conspicuous, as the hydration continues. The 28-day strength dropped by 40% as the Na_2CO_3 content increased from 5% to 15%.

Strength performance (50% GGBS)

Since the limestone content in this set of mixes was relatively low, the contribution of limestone might be less significant. The catalytic effect of Na_2CO_3 was also examined on mixes with GGBS:limestone = 1:1 (Figure 4-24). However, again, the 28-day UCS dropped by 60% from 37 MPa to 15 MPa.

There might be an increase in limestone consumption stimulated by Na_2CO_3, yet, the retardation effect of excess Na_2CO_3 override the increase in C-(A)-S-H from limestone.

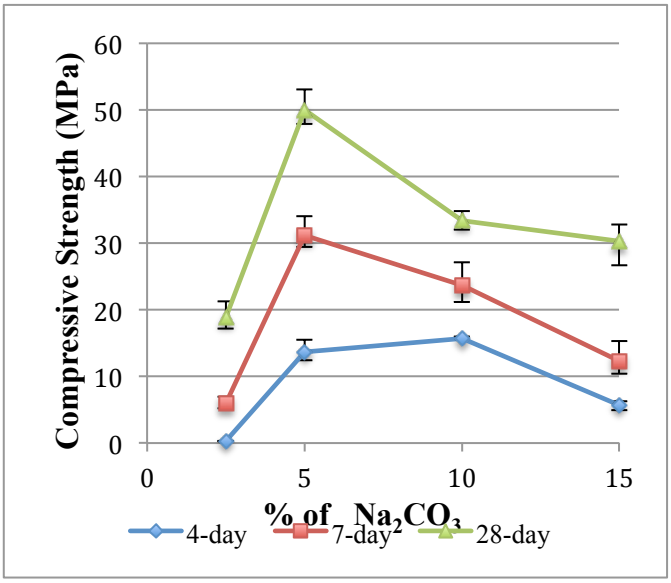

Figure 4-23 UCS as Na_2CO_3 replaces limestone at GGBS:L=4:1

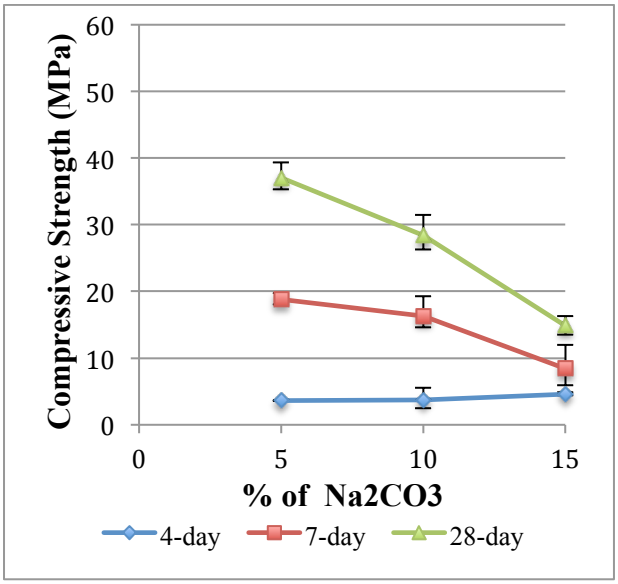

Figure 4-24 UCS as Na_2CO_3 replaces limestone at GGBS:L=1:1

Microstructure

Micrographs of NC15 (Figure 4-26) showed a dense distribution of microcracks as well as a more porous and rougher structure than S-L20 (Figure 4-10). This might be due to the gyrolite formation in excess alkalis, which swells and expands when in contact with water, as discussed in section 2.3. Hence, more cracking of paste matrix and a drop in UCS. Mixes with 15% Na_2CO_3 (NC15) had a significant higher amount of unreacted Na_2CO_3 in Figure 4-26(b) and (c) as well as GGBS in (d) after 28-day of curing. In Figure 4-26(c), Na_2CO_3 particles were covered by thin layer of CSH gel, yet no further development of CSH grains was seen. This was probably caused by the formation of thermonatrite and gaylussite. Materials remained unreacted and high density of microcraks were believed to be the causes of low compressive strength.

Figure 4-19 shows the XRD analysis of NC15 and S-L20, the hydration products found in NC15 and S-L20 were similar. Due to the overlapping of peaks for $CaCO_3$ and C-S-H, the contribution of limestone in strength by the formation of C-(A)-S-H cannot be quantified. Yet, XRD of NC15 did not show any peaks for C-A-H at ~ 11°(Figure 4-25). The lack of C-A-H was another cause of low strength. Upon calcination, weight loss in 28-day samples of NC15 was 33% less than that in S-L20. This suggests the retardation effect of Na_2CO_3

overrides the strength gain from the consumption of limestone stimulated by additional Na_2CO_3. As an improvement in strength was not achieved by increasing the Na_2CO_3 content, no shrinkage tests were performed on NC15 mixes. Yet, with low CSH content, lack of crystalline-phase compounds and dense distribution of microcraks, higher shrinkage would be expected as Na_2CO_3 dosage increases.

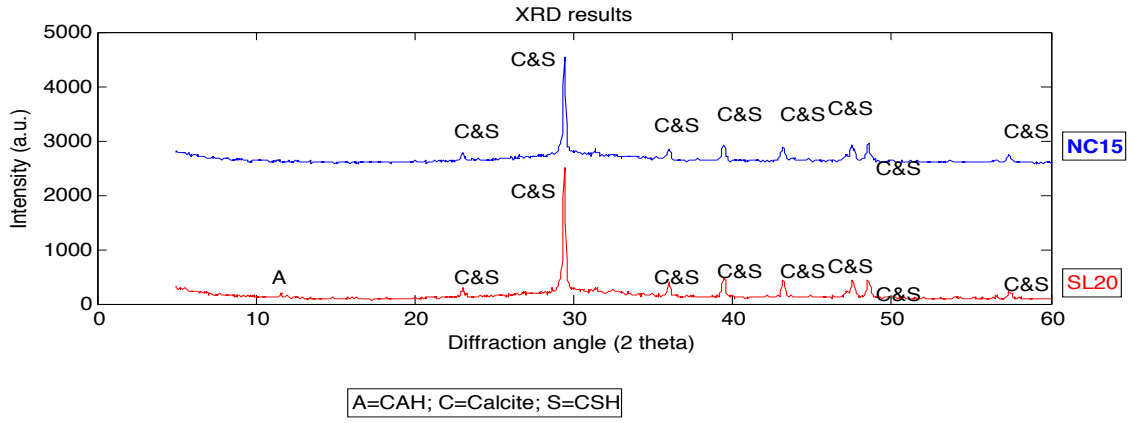

Figure 4-25 XRD results for NC15 and SL20

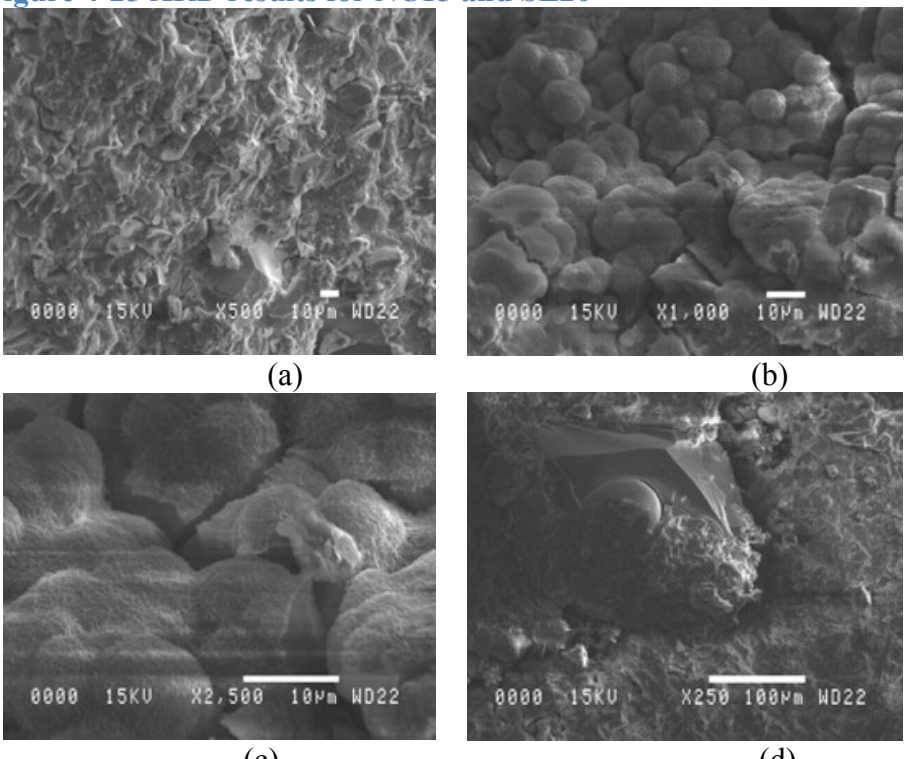

(a) (b)

(c) (d)

Figure 4-26 SEM analysis for NC15 (a) x500; (b) x1000; (c) x2500; (d) x250

4.1.3The effect of MgO addition

Previously in mid-term report, it was found that MgO addition reduces compressive strength, yet, MgO was added by replacing both slag and limestone. The drop in strength might be due to the dilution of slag. For more accurate comparison, the MgO test was repeated by replacing

limestone only. As reported by Haha et al (2011), higher MgO content in slag improved the strength at all ages, due to the formation of hydrotalcite-like phase hydration products M-A-H and M-S-H rather than $Mg(OH)_2$. This improves pore structure and gives more dense structure, as discussed in section 2.5. However, with the presence of limestone, the impact is unknown. The effect of MgO was tested on slag activated by two combinations of activators: 5% Na_2CO_3 and 1.5% NaOH + 3.5% Na_2CO_3.

4.1.3.1 In slag activated by 5% Na_2CO_3

Strength performance (80% GGBS)

One of the drawbacks of using Na_2CO_3 activators was the low early strength. As discussed in section 2.5, an increase in MgO content can improve early strength by stimulating higher hydration rate between 3 and 14 days, as well by a higher pH (Figure 4-28). Figure 4-27 gave an evidence 43% increase in 4-day strength upon 10% replacement of limestone by MgO. However, only 5% increase in 28-day strength was observed. The little late strength gain can be explained by the compensation of strength gain from the MAH formation, by the strength reduction due to 10% of limestone filler replacement. Therefore, the strength effect of MgO at late stage was limited.

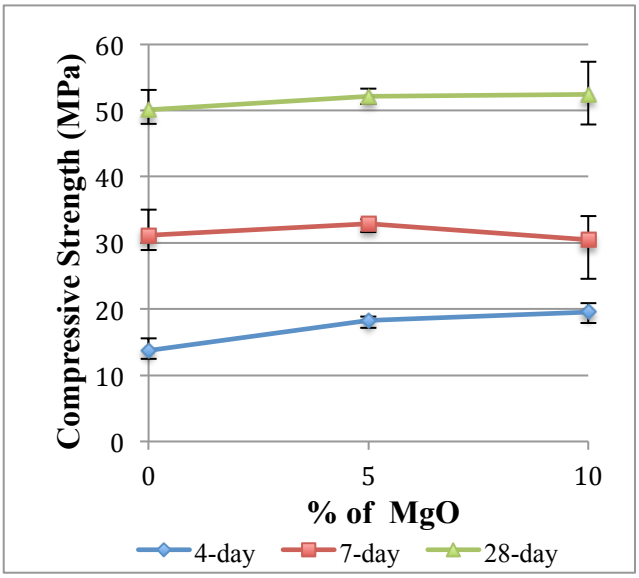

Figure 4-27 UCS of 5% Na_2CO_3 activated slag paste with 80%GGBS, MgO content varied

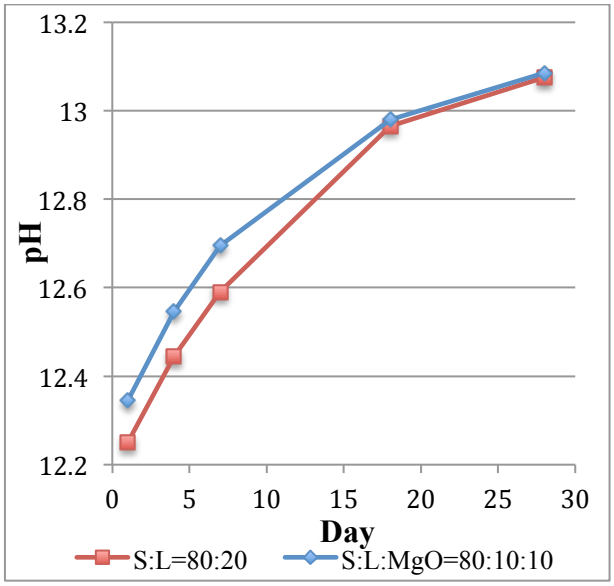

Figure 4-28 pH of 5% Na_2CO_3 activated slag paste with 80%GGBS, MgO content varied

Strength performance (50% GGBS)

In the previous set, only 10% MgO was added due to the need to maintain 80% of GGBS as well as a high volume of limestone. Therefore, mixes with 50% slag and the remaining as

limestone were also tested. Figure 4-29 shows 10% and 20% replacement of limestone by MgO led an increase in 28-day UCS by 16% to from 37 MPa to 43 MPa and 31% to 48 MPa respectively. Compared to mixes with 80% slag, the effect of MgO with only 50% slag was more pronounced. As it was shown in section 4.1.1.4, mixes with GGBS:limestone=50:50 had looser structure and denser distribution of microcracks than that with 80% GGBS. By adding MgO, the formation of expansive M-A-H filled the voids and more importantly enhancing crack width and lengths. The denser, more continuous and homogeneous structure definitely gave a higher UCS. Second, a high volume of limestone remained despite 20% replacement of limestone by MgO, hence, no reduction in limestone filler effect. As a result, a higher net gain in 28-day strength in mixes with 50% slag. The issue associated with up to 20% of MgO is the formation of expansive $Mg(OH)_2$ and M-A-H might lead to excessive expansive stress. Consequential cracking and spalling might occur in long run.

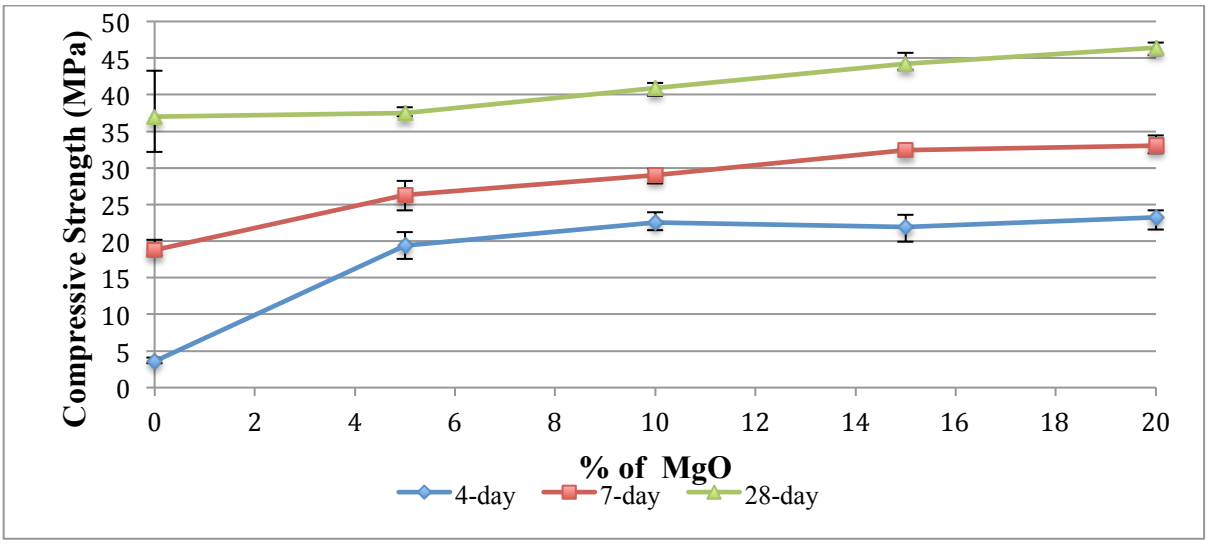

Figure 4-29 UCS of 5% Na_2CO_3 activated slag paste with 80%GGBS, MgO content varied

4.1.3.2 In slag activated by 1.5% NaOH & 3.5% Na_2CO_3

Strength performance (80% GGBS)

Since slag activated with 1.5% NaOH + 3.5% Na_2CO_3 yielded the highest UCS, this mix was also tested with the replacement of MgO. UCS results in Figure 4-30 shows MgO had negligible effect on early strength due to the high initial hydration rate under the presence of NaOH. The 10% replacement of limestone by MgO led to a less than 7% increase in 28-day compressive strength. The UCS at all ages were similar irrespective to the content of limestone and MgO in the cement mixes. Again, this suggests the strength gained from the improvement in pore structure and increase in hydration products MAH and $Mg(OH)_2$ was

compensated by the reduction of $Ca(OH)_2$ and the formation of more porous structure caused by the reduction in limestone filler.

Rather than being detrimental to strength in PC, the addition of MgO in GGBS and limestone led to an increase in UCS. Although the effect was limited in mixes with 80% GGBS, MgO is considered to be more influential in shrinkage performance.

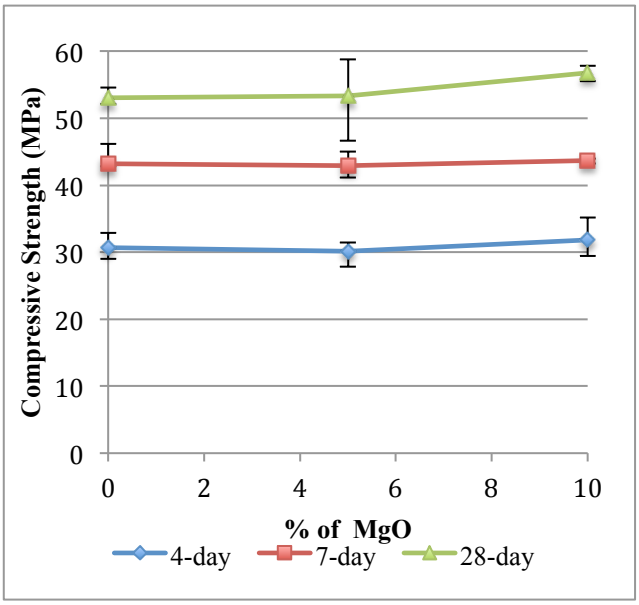

Figure 4-30 UCS of 1.5%NaOH+5%Na_2CO_3 activated slag paste with 80%GGBS, MgO content varied

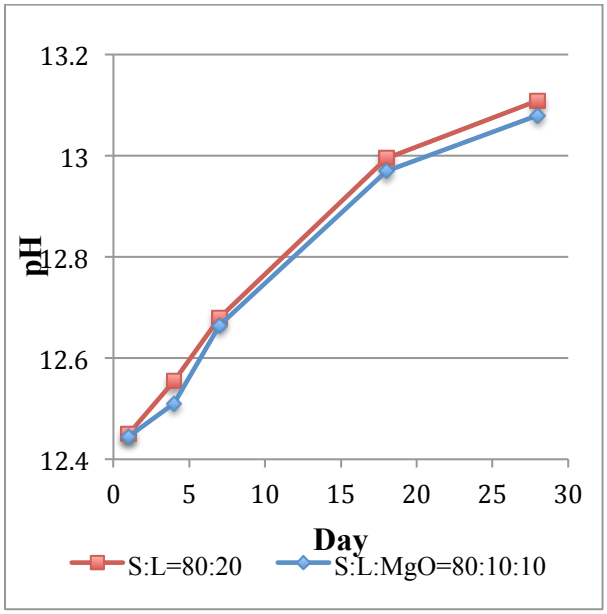

Figure 4-31 pH of 1.5%NaOH+5%Na_2CO_3 activated slag paste with 80%GGBS, MgO content varied

Drying Shrinkage performance

The addition of MgO in PC was proved to worsen drying shrinkage due to the formation of $Mg(OH)_2$ which is unable to fill voids. However, MgO impact on AAS and limestone mix was unknown. By visual inspection, only several fine surface cracks were identified after 24 hours of de-moulding, as shown in Figure 4-32. Figure 4-33 shows the addition of 10% MgO led to 24% reduction in 28-day strain. The improvement might be due to the formation of hydrocalcite MAH. As discussed in section 2.5, MAH is more capable in filling large pores than $Mg(OH)_2$. A reduction in total pore volume reduces shrinkage. Nonetheless, w/c ratio increases with MgO content, hence a drop in autogenous shrinkage and cracking. As shown in Figure 4-34, the 1-day weight loss for S-L20 and AM10 were 2.73% and 2.81% respectively and the trend remained very close over the 28 days. Similar water evaporation suggested pore structure improvement was the core reason for shrinkage improvement. Although the addition

of MgO improved the shrinkage performance, drying shrinkage was still 38% higher than the commercial blend B.

Figure 4-32 Very fine hair line surface cracking on 1-day with the addition of MgO

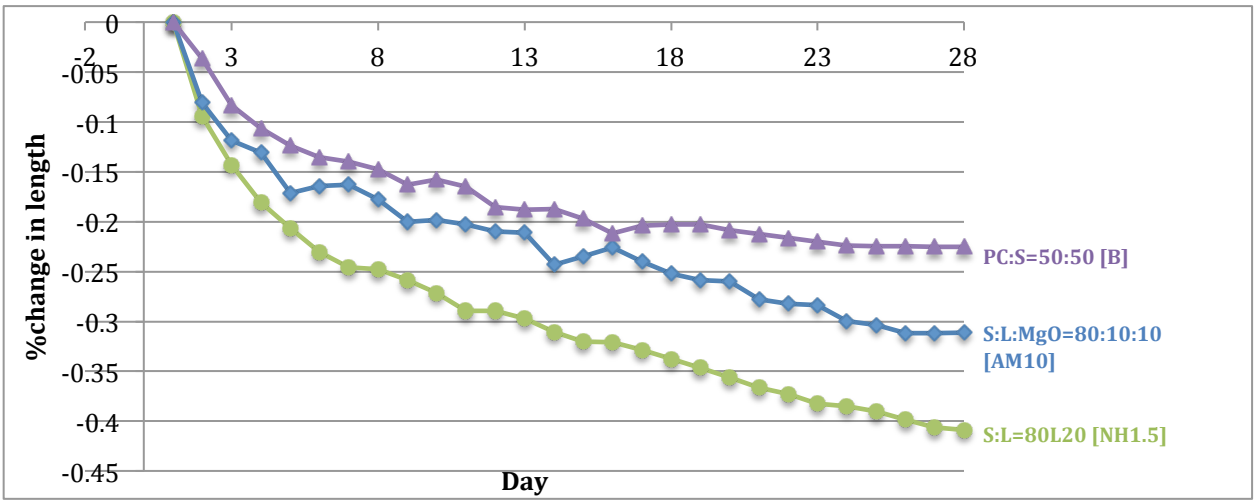

Figure 4-33 Drying strain development of 1.5%NaOH+3.5%Na_2CO_3 activated slag paste with 80%GGBS, MgO content varied

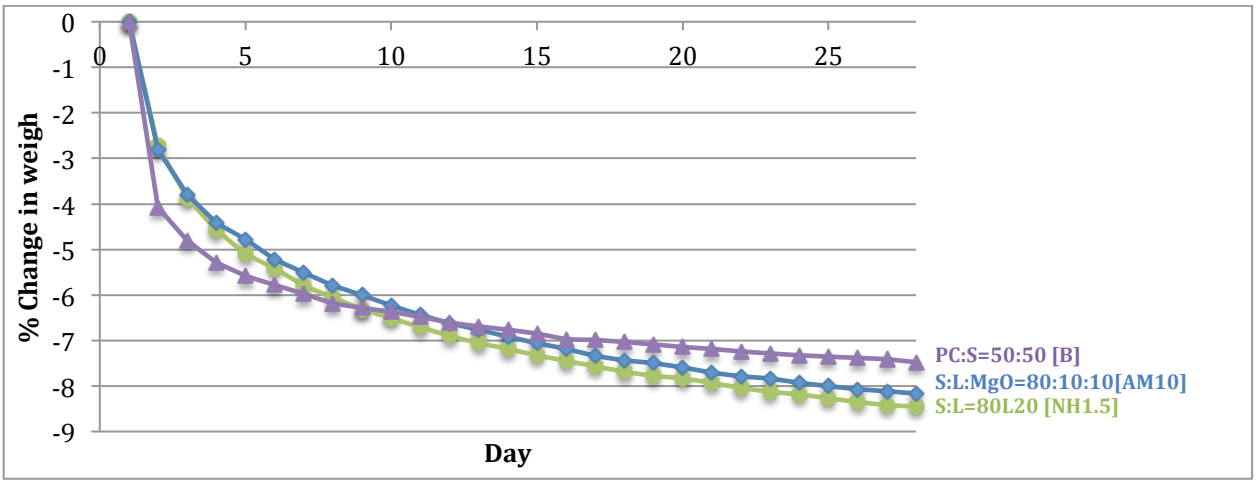

Figure 4-34 Drying weight loss of 1.5%NaOH+3.5%Na_2CO_3 activated slag paste with 80%GGBS, MgO content varied

Submerged Shrinkage performance

Upon submerging in water, shrinkage dropped to 1/5th of the drying value. Mixes with 80% slag activated with combination of had similar trend in stain development (Figure 4-35) and

weight change (Figure 4-36). However at 24 days and onwards, AM10 expanded more rapidly than NH1.5. This might be due to the continuous formation of expansive MAH. Although Li (2010) reported that MgO expansion rate slows after 14 days, the expansion does not stabilize until 150 days. Since the submerged shrinkage test stopped at 28day, there was insufficient information to tell to what extent the expansion will stop, nonetheless the expansion stress cannot be easily adjusted and controlled. Excessive expansion might lead to cracking in the cement pastes. Therefore, limiting MgO dosage control is critical to ensure safe improvement in shrinkage.

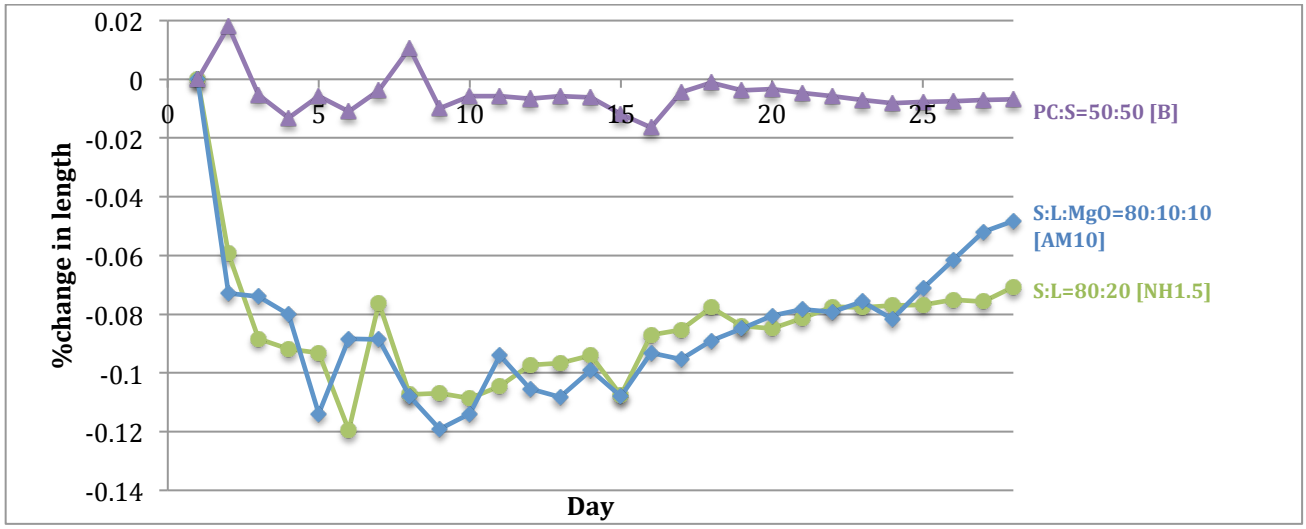

Figure 4-35 Submerged strain development of 1.5%NaOH+3.5%Na_2CO_3 activated slag paste with 80%GGBS, MgO content varied

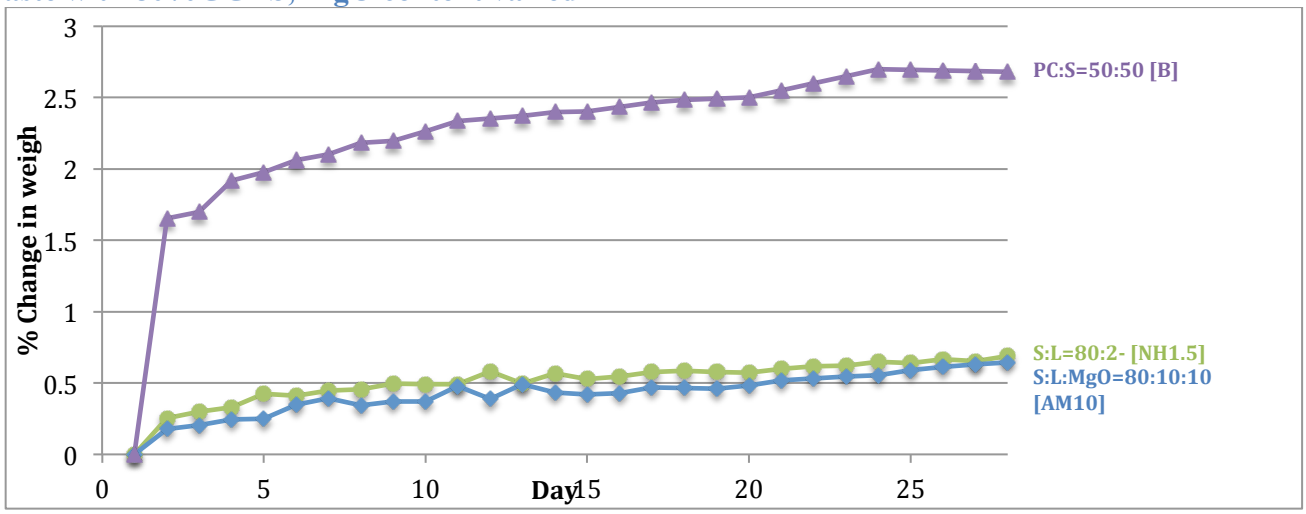

Figure 4-36 Submerged weight loss of 1.5%NaOH+3.5%Na_2CO_3 activated slag paste with 80%GGBS, MgO content varied

Microstructure analysis

Both M-S-H and M-A-H may form in AAS upon the addition of MgO, yet, it is difficult to detect their presence in XRD analysis as their peaks are immiscle with C-S-H and C-A-H respectively. Figure 4-27 showed an evidence increase in C-A-H/M-A-H upon the addition of MgO, as higher and boarder peaks were observed at ~11°. Additional peaks at ~38° and ~44° were evidences for the formation of $Mg(OH)_2$, and unreacted MgO respectively.

Since CSH, MSH and $CaCO_3$ all have overlapping peaks in XRD, furnace test provided more accurate information on the CSH content. AM10 and NH1.5 had 5.75% and 5.25% of weight loss respectively after 2 hours of calcination. Hence, the two mixes have similar CSH content, yet, no indication whether the Ca was sourced from slag or limestone.

SEM was performed on AM10 as shown in Figure 4-38. No microcracks were identified, which might be due to the formation of expansive M-A-H that filled the voids and microcracks by its volume. However, no $Ca(OH)_2$ hexagonal plates was seen, due to reduction in limestone content and small addition of NaOH. This suggested that 10% limestone is insufficient for the formation of $Ca(OH)_2$. Despite the absence of $Ca(OH)_2$, better shrinkage performance was still achieved. This suggests by increasing NaOH or limestone contain in this mix, further shrinkage improvement can be achieved.

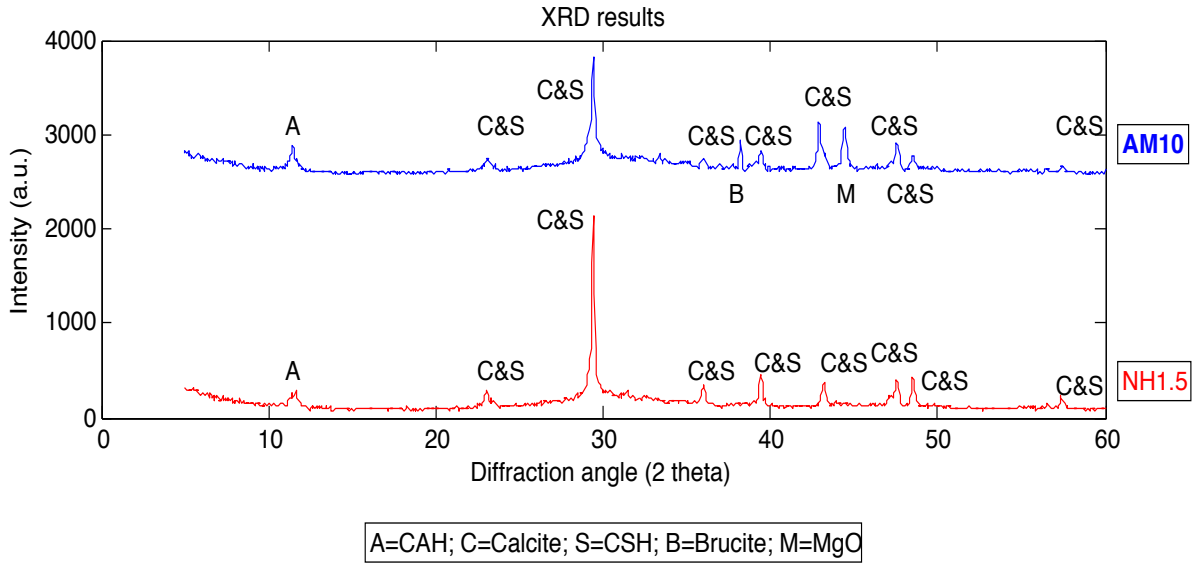

Figure 4-37 XRD analysis of AM10 and NH1.5

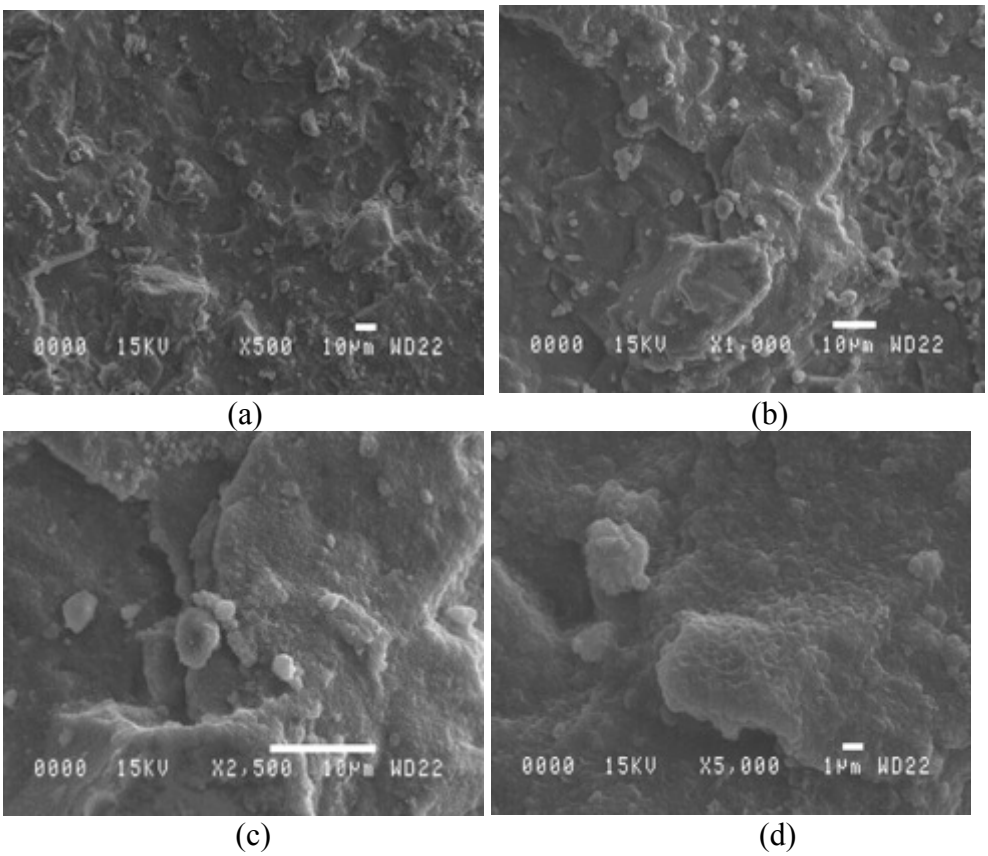

(a) (b)

(c) (d)

Figure 4-38 SEM analysis for AM10 (a) x;500 (b) x1000 (c) x2500 (d) x5000

4.2 Performance of slag-limestone blends in Concrete

The UCS of concrete composed of the three cements with the highest strength values was tested to investigate the strength values achieved. Mixes S-L20, NH1.5 and AM10 were examined, all containing slag:limestone at 4:1 ratio but the first only has Na_2CO_3 as the activator (concrete mix S-L20), the second had the Na_2CO_3 and NaOH mix (concrete mix NH5) and the third has both activators as well as MgO (concrete mix AM10). Figure 4-29 shows the UCS results of the concrete cubes, together with their corresponding cement cubes. The figures shows that the highest concrete strength was achieved by AM10 at 37.5 MPa and that the trend observed in the cement paste cubes were also observed in the concrete cubes. According to American Concrete Institute, high-strength concrete has a compressive strength >41 MPa and hence AM10, NH1.5 and S-L20 would be classified as medium-strength concrete, which are suitable for house floors, footpaths and driveways. However, by reducing w/c ratios or use of admixtures, 41 MPa can be easily attained and alternatively if a lower strength concrete is required, then reduced additives content could be used.

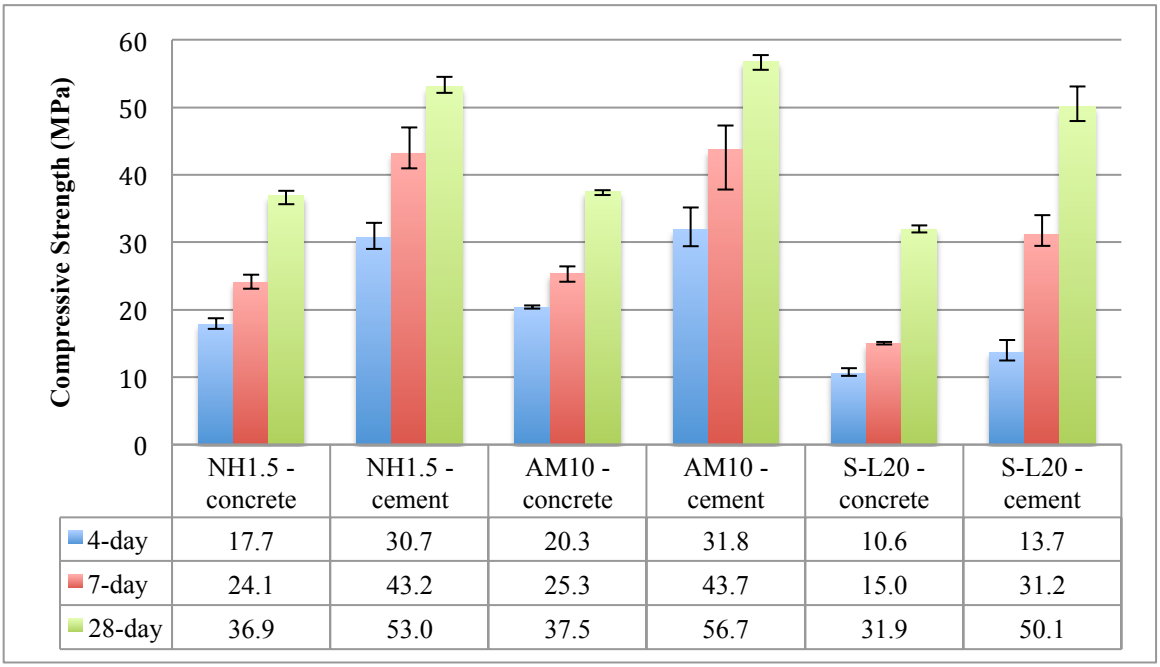

	NH1.5 - concrete	NH1.5 - cement	AM10 - concrete	AM10 - cement	S-L20 - concrete	S-L20 - cement
4-day	17.7	30.7	20.3	31.8	10.6	13.7
7-day	24.1	43.2	25.3	43.7	15.0	31.2
28-day	36.9	53.0	37.5	56.7	31.9	50.1

Figure 4-39 Concrete and cement compressive strength of selected mixes

5 Conclusions & recommendations for future work

5.1 Conclusion

Portland cement was extensively used in the construction industry, yet its highly unsustainable nature stimulated the urge for comparable alternatives. AAS was identified to be the best substitute; yet, its annual production is only 250 million tonnes which is far below the current global annual cement consumption of 3.6 billion tonnes. The addition of the abundant limestone into Portland cement has been widely-used in the industry. The role of limestone in AAS is yet to be understood, hence, the motives for this research. The literature review summarized the properties of each material used in this research work, and the possible reaction upon mixing and hydration. The chapter also introduced the addition of MgO into AAS to improve mechanical properties and durability, as oppose to its detrimental effect in PC.

In Chapter 4, the results showed that replacing 20% of GGBS by limestone yielded a 28-day compressive strength similar to that without limestone, as the better packing attributed by the limestone fillers was sufficient to compensate the dilution effect from 20% slag replacement. As the limestone content continued to increase, both early and later strength dropped due to the lack of CSH. The drop in strength might also be due to the increase in microcracks density with limestone content. Since Na_2CO_3 was a mild activator, limestone only acted as inert filler. In the context of durability, 20% and 50% replacement of GGBS by limestone led to 19% and 64% increased in strain in drying conditions respectively. Upon submerging in water, the strain dropped by 90%, yet, still significantly higher than the shrinkage of commercial blended cement.

5% NaOH activated slag gave higher early strengths at all GGBS:limestone ratios, but yielded lower late strengths due to the lack of Na_2CO_3 to catalyse the uptake of limestone and form more porous structure. However, as 50% of slag was replaced by limestone, the reduction in compressive strengths for NaOH- and Na_2CO_3- activated slag were 18.5% and 26.9% respectively. First, due to the more porous structure of NaOH activated slag, the filling effect of limestone powder was more profound. Secondly, under the presence of NaOH, strength contributing and shrinkage restraining crystalline $Ca(OH)_2$ was formed from $CaCO_3$ in limestone. The drying shrinkage of 5% NaOH activated slag with GGBS:L=80:20 had a 28-day strain 76% smaller than that of Na_2CO_3 activated slag, and it was better than mixes with

100%GGBS activated with NaOH; further, its drying shrinkage performance was better than the commercial cement CEMIII.

A combination of activator was tested on mixes with 80% slag and the remaining as limestone. and it was proved to yield higher strength at all ages than slag active with NaOH or Na_2CO_3 alone - the 28-day strength was 6% and 32% higher than that with 5% Na_2CO_3 or NaOH alone, since both $Ca(OH)_2$ was formed and Ca was consumed from limestone. The 1.5% replacement of Na_2CO_3 by NaOH reduced the 28-day drying shrinkage by 47%, yet, its shrinkage remained 80% higher than commercial cement blend B.

Moseson (2012) suggested that Na_2CO_3 catalysed the formation of C-(A)-S-H by consuming Ca from limestone. However, experimental work showed that the retarding effect of Na_2CO_3 overrides the strength gain from the limestone consumption. 28-day strengths drop as high as 60% were seen upon 10% addition of Na_2CO_3.

The effect of MgO on AAS and limestone mixes was difference from that in PC. It were tested on mixes with 80% slag and the remaining as limestone. In Na_2CO_3 activated-slag, 4-day compressive strength gained by 43% upon 10% MgO addition, yet, little impact on later strength, irrespective to activators types. It might be due to the compensation of strength gain from the formation of M-A-H by the strength reduction caused by worse packing effect as less limestone filler contained. Compared to 80% slag content, the effect of MgO was more significant in mixes with 50% slag, as excessive limestone filler was presence. In the context of drying shrinkage, 24% reduction in 28-day drying strain was observed, due to the formation of expansive M-A-H and improvement in pore structure. However, in wet condition, the effect of MgO was insignificant as external water could be drawn for hydration of CSH to prevent collapsing.

Three mixes with higher UCS in cement pastes were tested in concrete form, and the highest UCS attained was 37.5 MPa, which was only slightly below ACI standard of high-strength concrete – 41 MPa.

This work highlighted that the incorporation of high volume limestone in alkali-activated slag is viable and beneficial depending on the nature and dosage of activators, in the context of mechanical strength and durability. These formulations are encouraging as they have a substantial reduction in carbon dioxide emission and costs, by up to 97% (Moseson 2012).

5.2 Recommendations for future work

The study performed could be expanded and further possible investigation areas include:

- In this research, cement and concrete mixes were tested on their 28-day performance. Mature performance has not been examined. One of the effective way to increase concrete sustainability is to extend effective service life. Therefore, test on mixes should be extended to at least 90 days is recommended.
- Use of Mercury Intrusion Porosimetry (MIP) tests to obtain nformation on pore distribution and total porosity, so as to verify the impact of filling effect quantitatively. The effect of pore structures as discussed in this project purely based upon previous researches and theoretical influences.
- Extensive combinations of activators, including water-glass, lime, NaOH and Na_2CO_3, should examined, to determine if impact of chemical reaction between alkalis and $CaCO_3$.
- Due to the overlapping of most hydration and unreacted materials in XRD analysis, more detailed microstructure analysis is recommended to examine the composition of each hydration product. This is critical in determining if calcium ions in $CaCO_3$ acted as one of sources of Ca for CSH.
- Test on mixes with lower water-to-cement ratios, lower aggregates-to-cement ratios or the use of additives to increase concrete UCS to the desire range for high-strength concrete.

5.3 Risk assessment

Risk assessment was conducted and approved by the Health & Safety Office before the experimental works. The risk assessment performance had well-reflected the actual hazards which were encountered. The precaution measures were strictly followed as described in the assessment. No accidents occurred or reported throughout the experiments.

6 References

P.Aitcin, M Sidney. Sustainability of Concrete (Modern Concrete Technology), 2011, CRC Press

K.Sakai, T. Noguchi. The sustainable use of concrete, 2012, CRC Press

Cement and Concrete Institute. Sustainable Concrete, 2011.

F. Collins and J.G. Sunjayan. Early age strength and workability of slag pastes activated by NaOH and Na_2CO_3, Cement and Concrete Research, 28, No.5, 1998, 655-664

M.A. Cincotto, A.A. Melo, W.L.Repette. Effect of difference activators type and dosages and relation to autogenous shrinkage of activated blast furnace slag cement, 2007

A.A. Melo, M.A. Cincotto, W.L. Reptte. Drying and autogenous shrinkage of pastes and mortars with activated slag cement, Cement and Concrete Research, 38, 2998, , 565-574

C.D. Atia, C.Cilim, O.Celik, O. Karahan. Influence of activator on the strength and drying shrinkage of alkali-activated slag mortar, Construction and Building Materials, 23, 1, 2009, 548-555

Environmental Agency. Blast furnace slag (BFS) – A technical report on the manufacturing of blast furnace slag and material status in the UK, 2007

A.A.Adam. Strength and durability properties of Alkali activated slag and fly-ash-based geopolymer concrete, Aug 2009, Doctor thesis, RMIT University, Australia

ACI Committee. Ground granulated blast furnace slag as a cementitious constituent in concrete, 2000

Mineral Products Association (MPA). Fact sheet 18 – Embodied CO2e of UK cement, additious and cementitious material, 2011

Y.Senhadji, M. Mouli, H.Khelafi, A.S. Benosman. Sulphate attack of Algerian cement based material with crushed limestone filler cured at different temperatures, 2010

K.D. Ingram and K.E. Daugherty. A review of limestone additions to Portland cement and concrete, Cement and Concrete Research, 13, 1991, 165-170

P. Hawkins, P. Tennis and R. Detwiler. The use of limestone in Portland cement: A state-of-the-art review, 2003

P.Pipilikaki, M.Beazi-Katsioti. The assessment of porosity and pore size distribution of limestone Portland cement pastes, Construction and Building Materials, 23, 2009, 1966-1970

P. Kliegel, R. Douglas. Carbonate additions to cement, 1990, American society for testing and materials

M.B.Haha, B.Lothenbach, G.Le Saout, F. Winnefeld. Influence of slag chemistry on the hydration of alkali-activated blast-furnace slag – Part I: Effect of MgO, Cement and Concrete Research, 41, 2011, 955-963

F.X.Li, Y.Z.Chen and S.Z.Long. Influence of MgO expansive agent behavior of cement pastes and concrete, 2009

X.Li. Mechanical properties and durability performance of reactive magnesia cement concrete, 2012, University of Cambridge doctor thesis

F Puertas, S Martinez-Ramirez, S Alonso, T Vazquez. Alkali-activated fly ash/slag cements: Strength behavioue and hydration products, Cement and Concrete Research, 30, 10, 2000, 1625-1362

S.D.Wang, X.C.Pu, K.L.Scrivener and P.L.Pratt. Alkali-activated slag cement and concrete: a review of properties and problems, Advances in Cement Research, 7, 27, 1995, 93-102

F.Collins, J.G.Sanjayan. Cracking tendency of alkali-activated slag concrete subjected to restrained shrinkage, Cement and Concrete Research, 30, 5, 2000, 791-798

M. Palacios and F. Puertas. Effect of shrinkage-reducing mixtures on the properties of alkali-activated slag mortars and pastes, Cement and Concrete Research, 37, 2007, 691-702

C.Shi. Strength, pore structure and permeability of alkali- activated slag mortars, Cement and Cement Research, 26, 12, 1996, 1789-1799

V.V.Reddy, H.S.Rao and K.N.Jayaveera. Influence of strong alkaline substances (sodium carbonate and sodium bicarbonate) in mixing water on strength and setting properties of concrete, Indian Journal of Engineering & Material Science, 13, 2006, 123-128

T.Bakharev, J.G.Sanjayan, Y.B.Cheng. Effect of admixtures on properties of alkali-activated slag concrete, Cement and Concrete Research, 30, 2000, 1367-1374

S.D.Wang, K.L.Scrivener and P.L.Pratt. Factors affecting the strength of alkali-activated slag, Cement and Concrete Research, 24, 6, .1033-1043

C. Jolicoeur, M.A. Simard, T.C. To J. Sharman.Proceedings of the International Conference on Advances in Concrete Technology, 471, 1992

A.J.Moseson, D.E.Moseson, M.W.Barsoum.High volume limestone alkali- activated cement developed by design of experiment, Cement and Concrete Composites 34, 2012, 328-336

F.Pacheco-Torgal, J.Castro-Gomes, S.Jalali. Alkali-activated binders: A review. Part 1. Historical background, terminology, reaction mechanisms and hydration products, Construction and Building Materials, 22, 7, 2008, .1305-1314

F.Pacheco-Torgal, J.Castro-Gomes, S.Jalali. Alkali-activated binders: A review. Part 2. About materials and binders manufacture, 22, 7, 2008, .1315-1322

C.Li, H Sun, L Li. A review: The comparison between alkali-activated slag (Si+Ca) and metakaolin (Si+Al) cements, Cement and Concrete Research, 40, 9, 2010, 1341-1349

A.Fernandez-Jimenez, A.Palomo and D.Revuelta. Alkali-activation of industrial by-products to develop new earth-friendly cements, Proceeding of the 11th International Conference on Non-conventional materials and technologies, 2009, Bath, UK